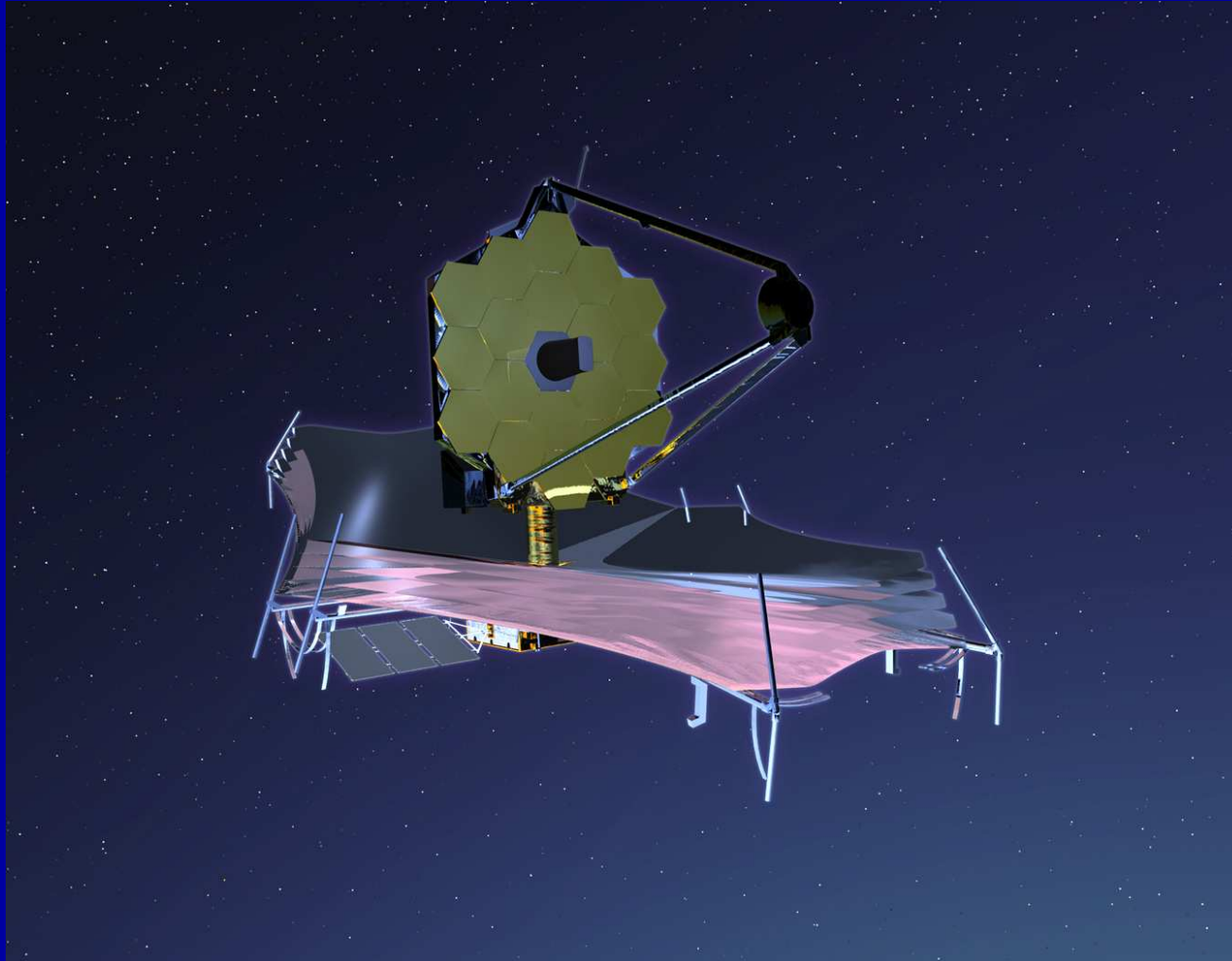


How can the James Webb Space Telescope measure First Light, Reionization, and Galaxy Assembly?

Rogier Windhorst (ASU) & the JWST Flight Science Working Group

Collaborators: S. Cohen, R. Jansen (ASU), C. Conselice & H. Yan (Caltech)

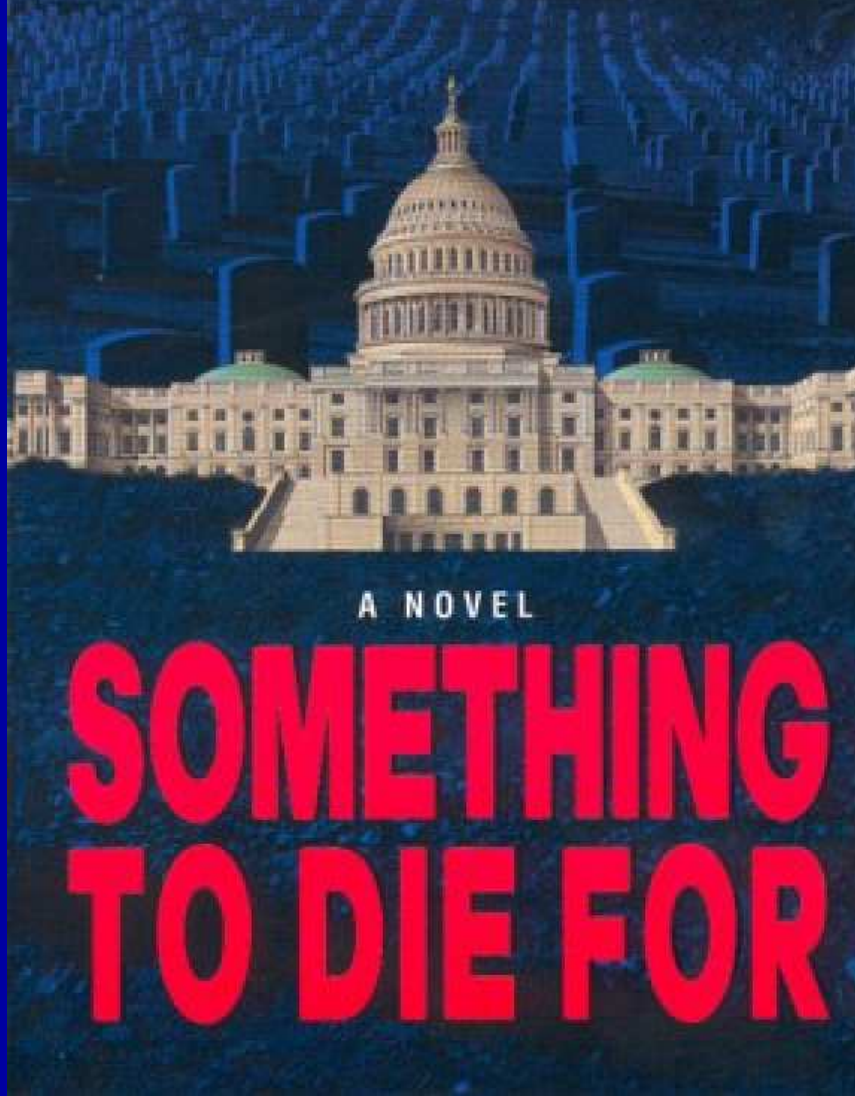


“First Light” Conference, May 20, 2005, UC Irvine

"Brilliantly done...breathtaking in its vision."
The New York Times

JAMES WEBB

Author of *The Emperor's General*



Need hard-working grad students & postdocs in $\gtrsim 2011$... It'll be worth it!

Outline

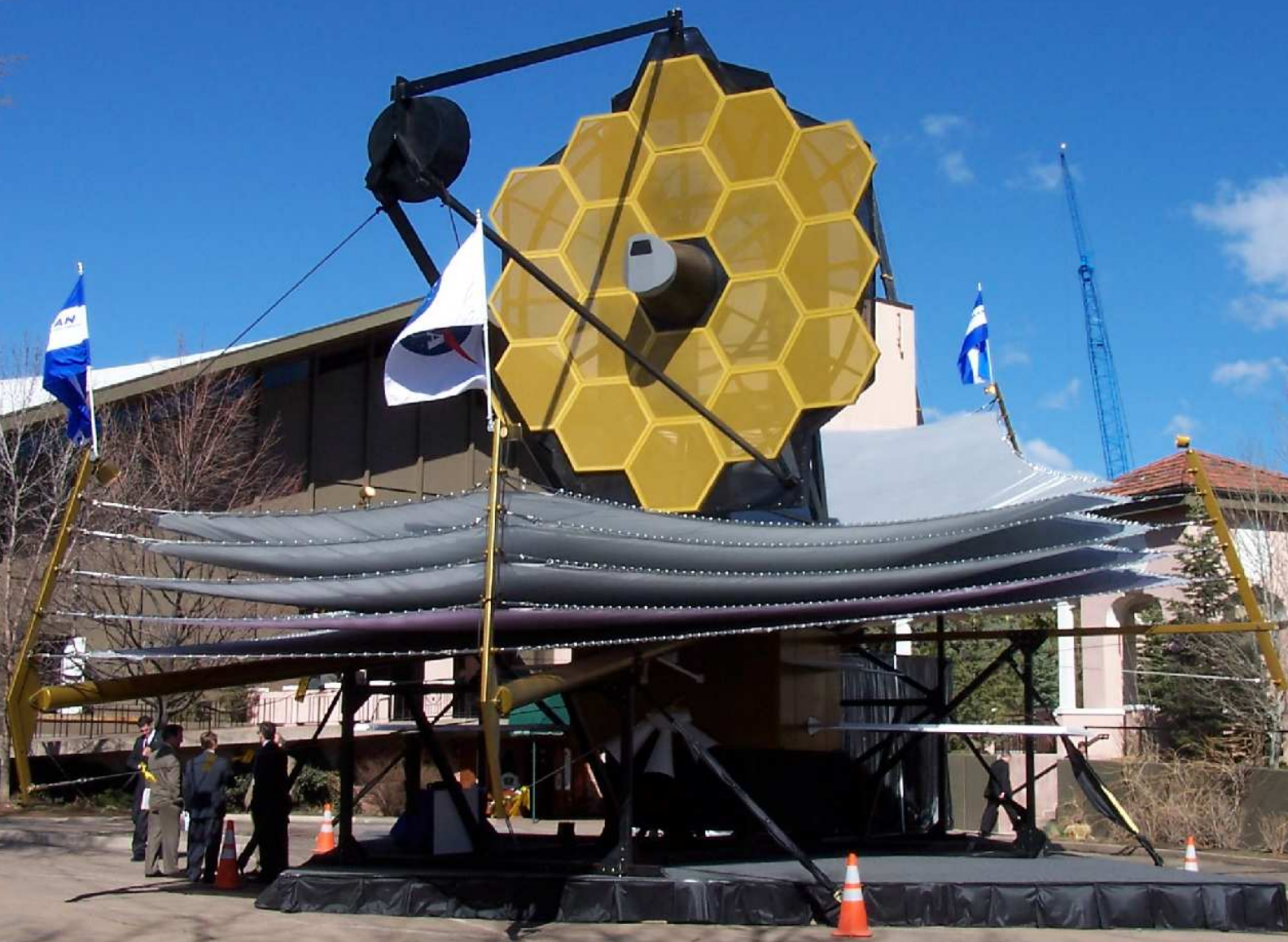
- (1) What is JWST and how will it be deployed?
- (2) What instruments and sensitivity will JWST have?
- (3) How JWST can measure First Light and Reionization
- (4) How JWST can measure Galaxy Assembly
- (5) Predicted Galaxy Appearance for JWST at $z \simeq 1-15$

Sponsored by NASA/JWST

- (1) What is the James Webb Space Telescope (JWST)?



- A fully deployable 6.5 meter (25 m^2) segmented IR telescope for imaging and spectroscopy from $0.6\mu\text{m}$ to $28\mu\text{m}$, to be launched by NASA $\gtrsim 2011$. It has a nested array of sun-shields to keep its ambient temperature at 35-45 K, allowing faint imaging ($\text{AB} \lesssim 31.5$) and spectroscopy ($\text{AB} \lesssim 29$ mag).



A life-sized model of JWST, used to test the deployment of its sun-shield.

- (1) How will JWST travel to its L2 orbit?

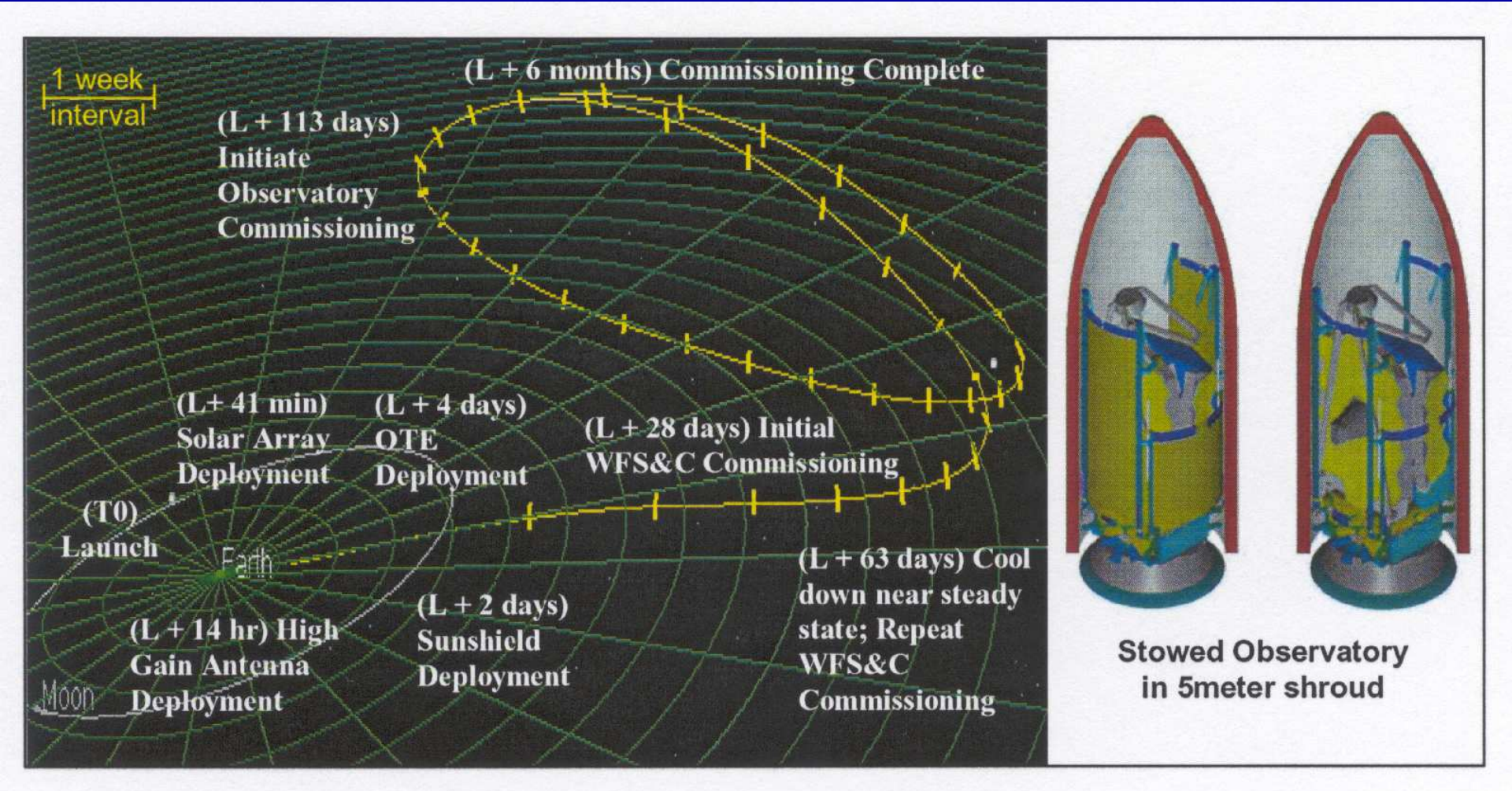
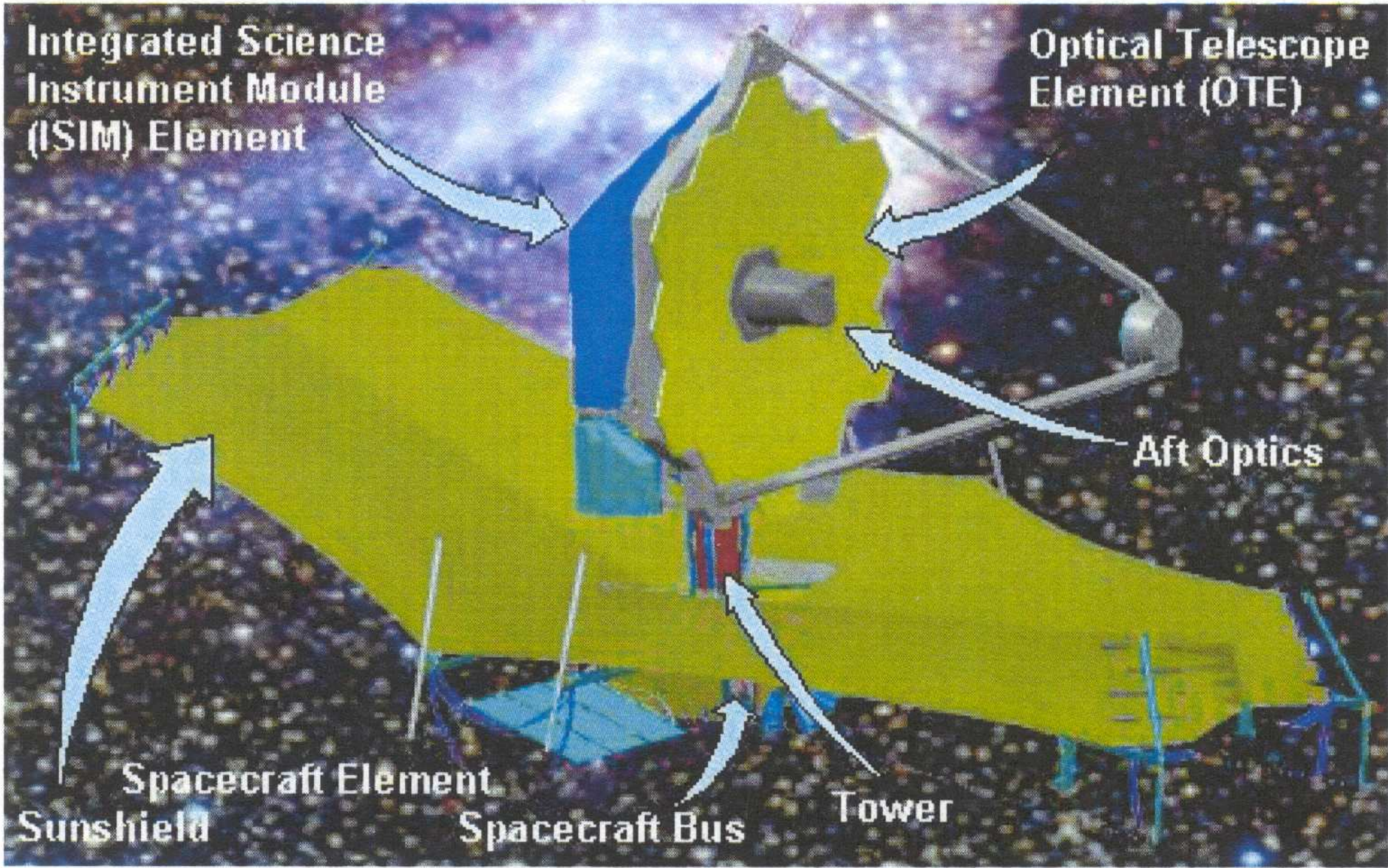
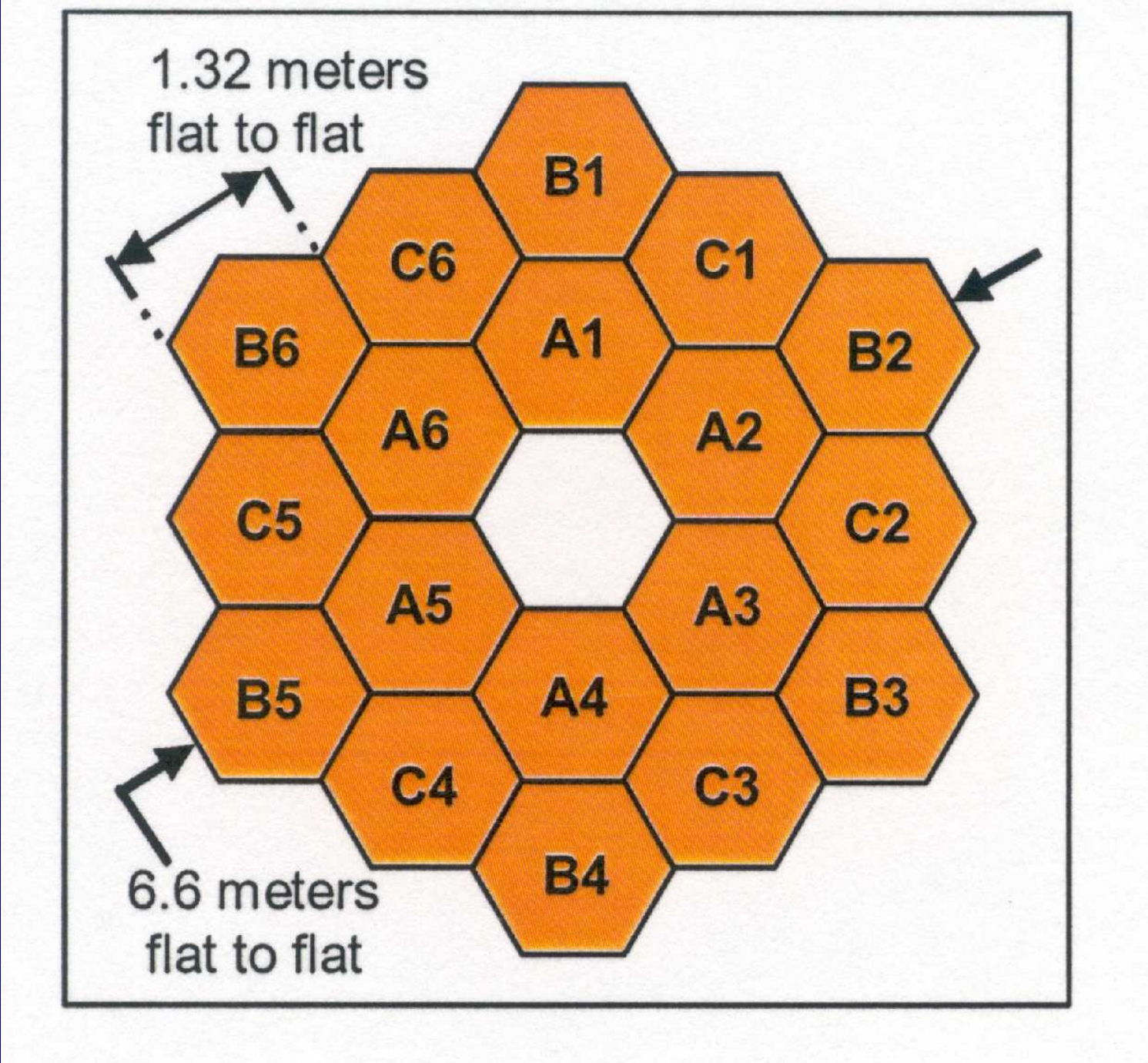


Figure 52. JWST orbit and trajectory to L2, and stowed view in 5 meter shroud.

After launch in \gtrsim 2011 with an Ariane V vehicle, JWST will orbit around the the Earth–Sun Lagrange point L2. From there, JWST can cover the whole sky in segments that move along in RA with the Earth, have an observing efficiency \gtrsim 70%, and send data back to Earth every day.





Edge-to-edge diameter is 6.60 m, but effective circular diameter is 5.85 m.
Cannot cleanly descope aperture without doing major harm to PSF.

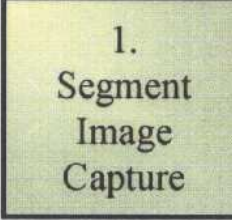
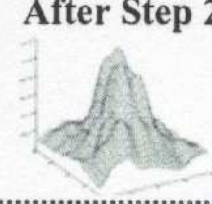
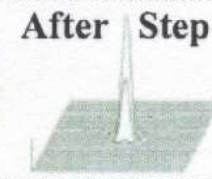
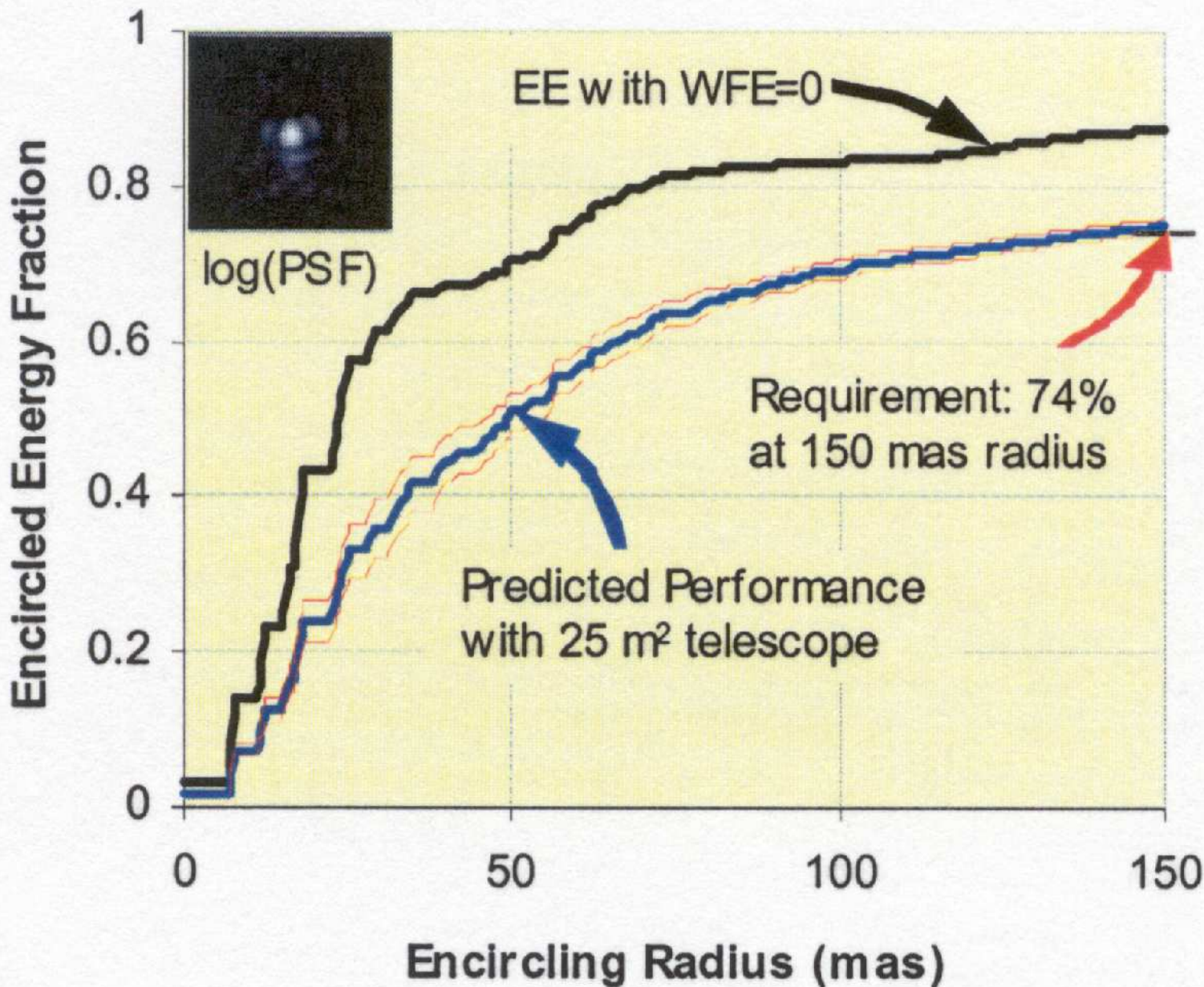
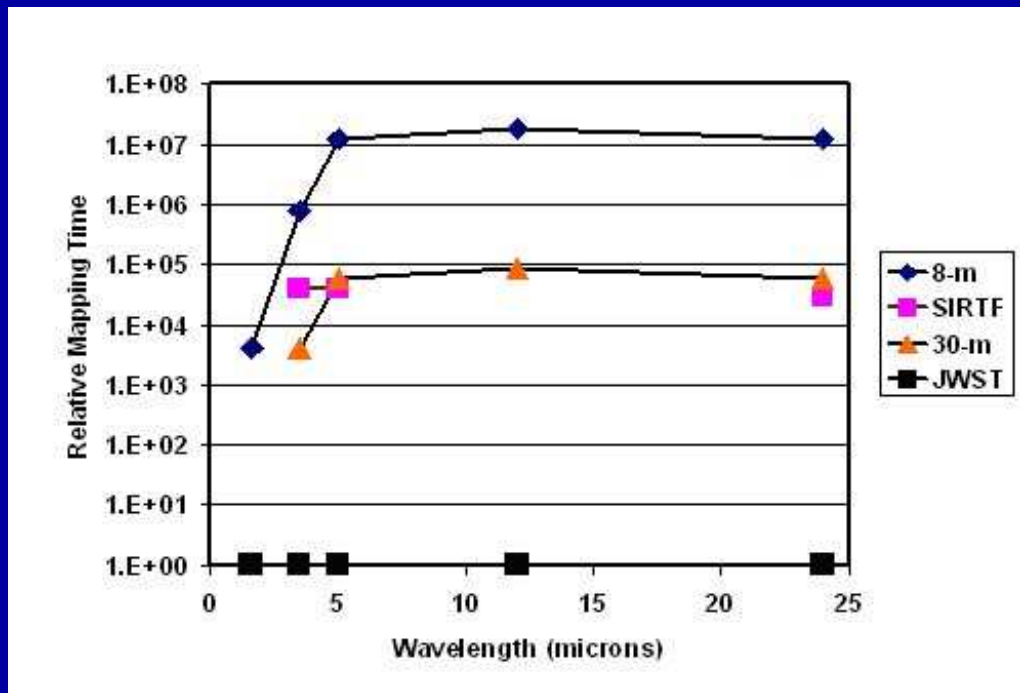
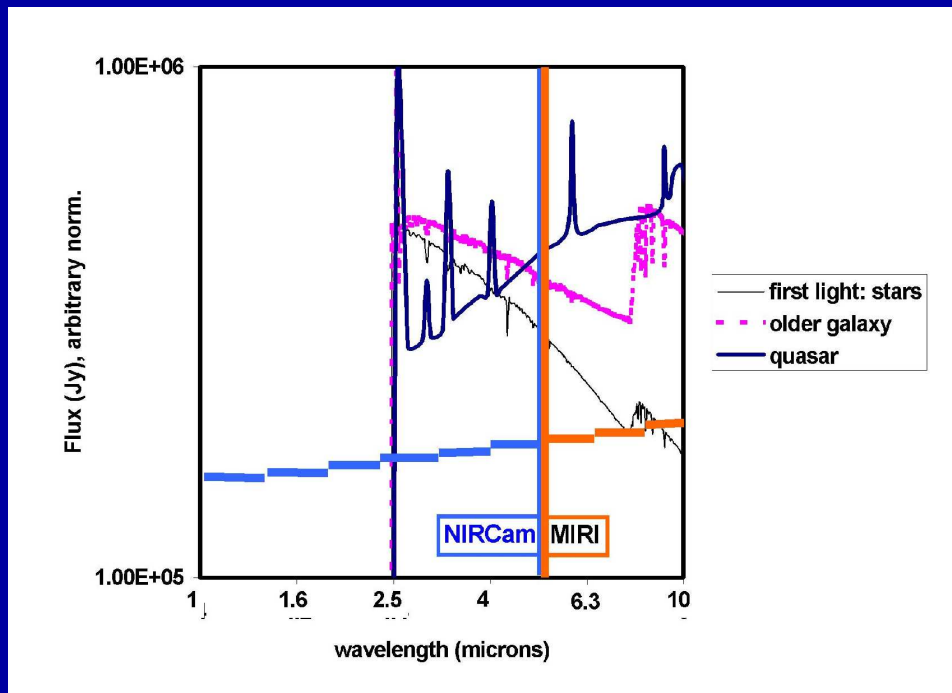
| <i>First light NIRCam</i> | <i>After Step 1</i> | <i>Initial Capture</i> | <i>Final Condition</i> |
|-----------------------------------------------------------------------------------|----------------------------------------------------------------------------------------------------------------------|------------------------------------------------------------------------------------------------------------------------------------|--------------------------------------------------------------------------------------------|
|  |  1. Segment Image Capture | 18 individual 1.6-m diameter aberrated sub-telescope images PM segments: < 1 mm, < 2 arcmin tilt SM: < 3 mm, < 5 arcmin tilt | PM segments: < 100 μm , < 2 arcsec tilt SM: < 3 mm, < 5 arcmin tilt |
| 2. Coarse Alignment Secondary mirror aligned Primary RoC adjusted |  After Step 2 | Primary Mirror segments: < 1 mm, < 10 arcsec tilt Secondary Mirror : < 3 mm, < 5 arcmin tilt | WFE < 200 mm (rms) |
| 3. Coarse Phasing - Fine Guiding (PMSA piston) |  After Step 3 | WFE: < 250 μm rms | WFE < 1 μm (rms) |
| 4. Fine Phasing |  After Step 4 | WFE: < 5 μm (rms) | WFE < 110 nm (rms) |
| 5. Image-Based Wavefront Monitoring |  After Step 5 | WFE: < 150 nm (rms) | WFE < 110 nm (rms) |

Figure 38. WFS&C commissioning and maintenance.



- (2) What sensitivity will JWST have?



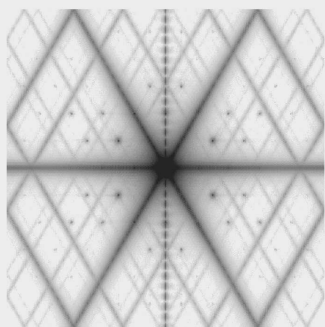
The NIRCam and MIRI sensitivity complement each other straddling $5\mu\text{m}$ wavelength, and together allow objects to be found to redshifts $z=15-20$ in $\sim 10^5$ sec (28 hrs) integration times.

The left panel shows the NIRCam and MIRI broadband sensitivity to a Quasar, a “First Light” galaxy dominated by massive stars, and a 50 Myr “old” galaxy, all at $z=20$. The right panel shows the relative survey time versus wavelength that Spitzer, a ground-based IR-optimized 8-m (Gemini) and a 30-m telescope would need to match JWST.

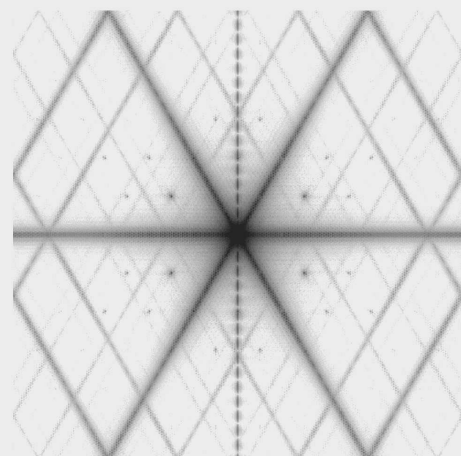


240 hrs HST/ACS in V / z' in the Hubble UltraDeep Field (HUDF)

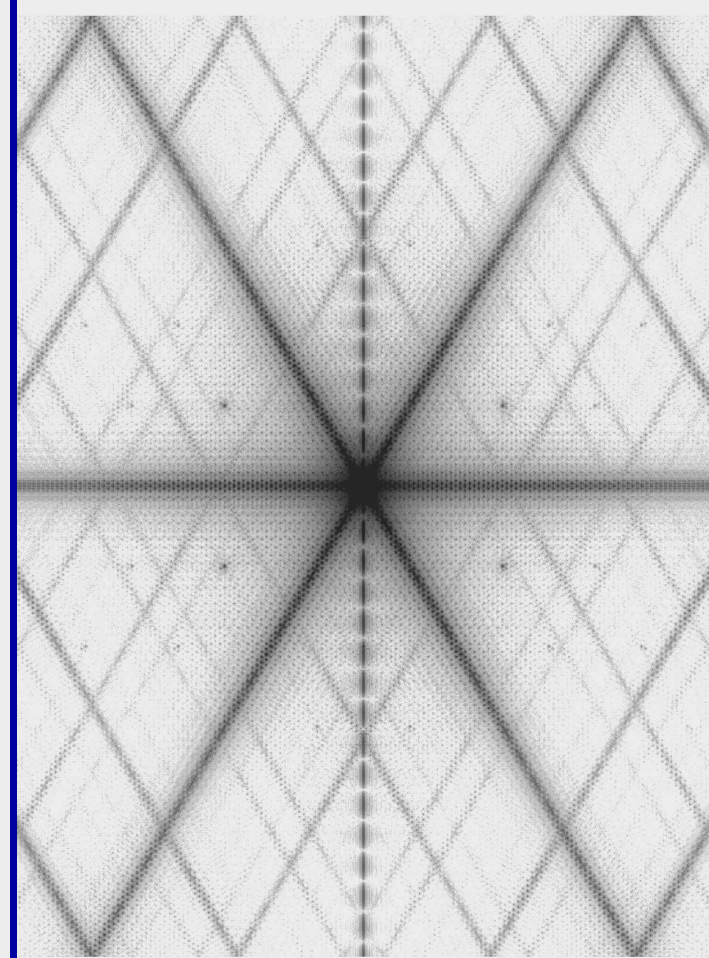
6.5m JWST PSF models (Ball Aerospace and GSFC):



NIRCam 0.7 μm



1.0 μm (<150 nm WFE)



2.0 μm (diffr. limit)

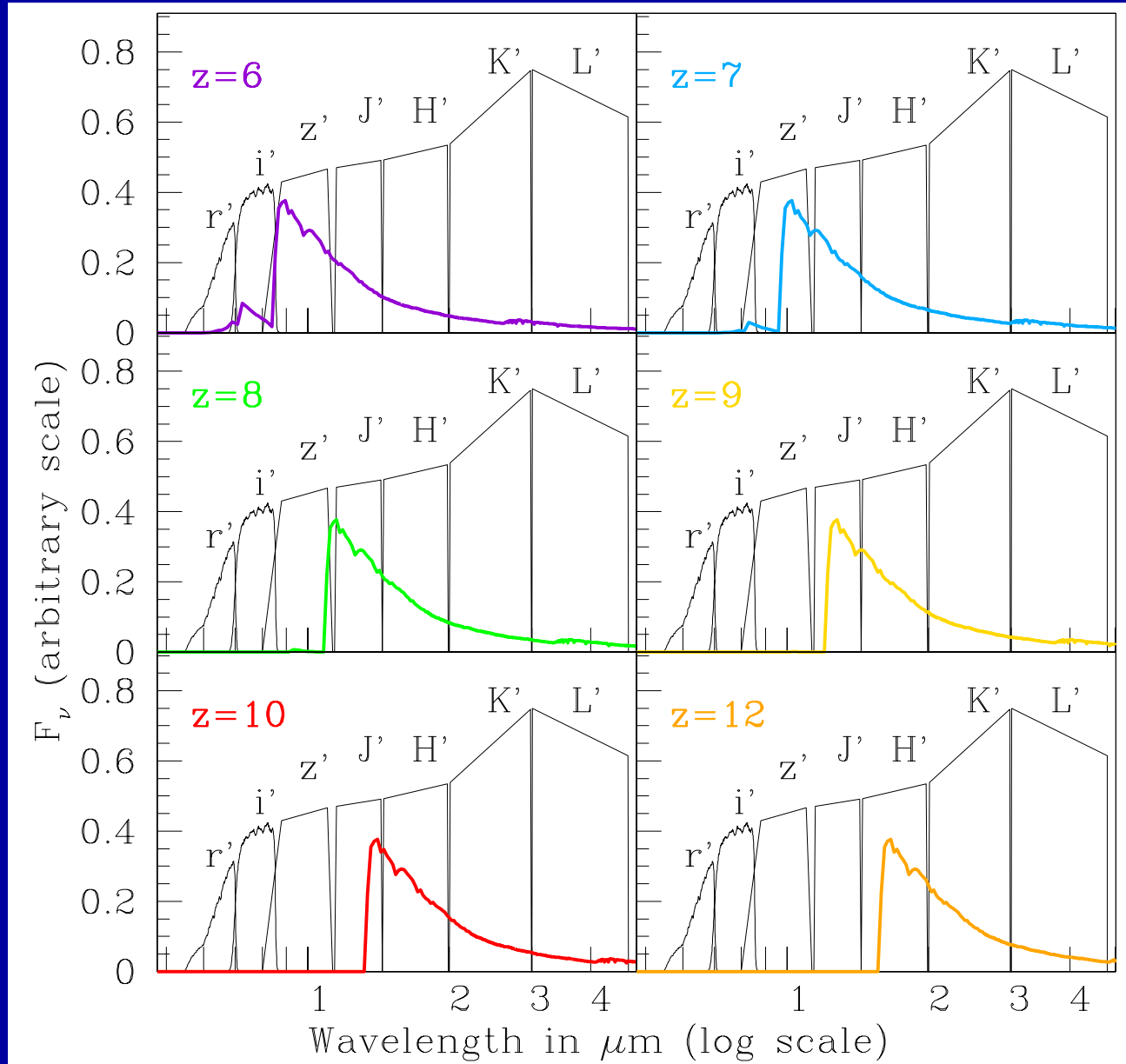


\lesssim 20 hrs JWST NIRCam at 0.7, 0.9, 2.0 μm in the HUDF



≡Truth (= HUDF Vi'z')

≤20 hrs JWST 0.7, 0.9, 2.0 μ m



- Can't beat redshift: to see First Light, must observe near-mid IR.
⇒ This is why we need NIRCam at 0.8–5 μm and MIRI at 5–28 μm .



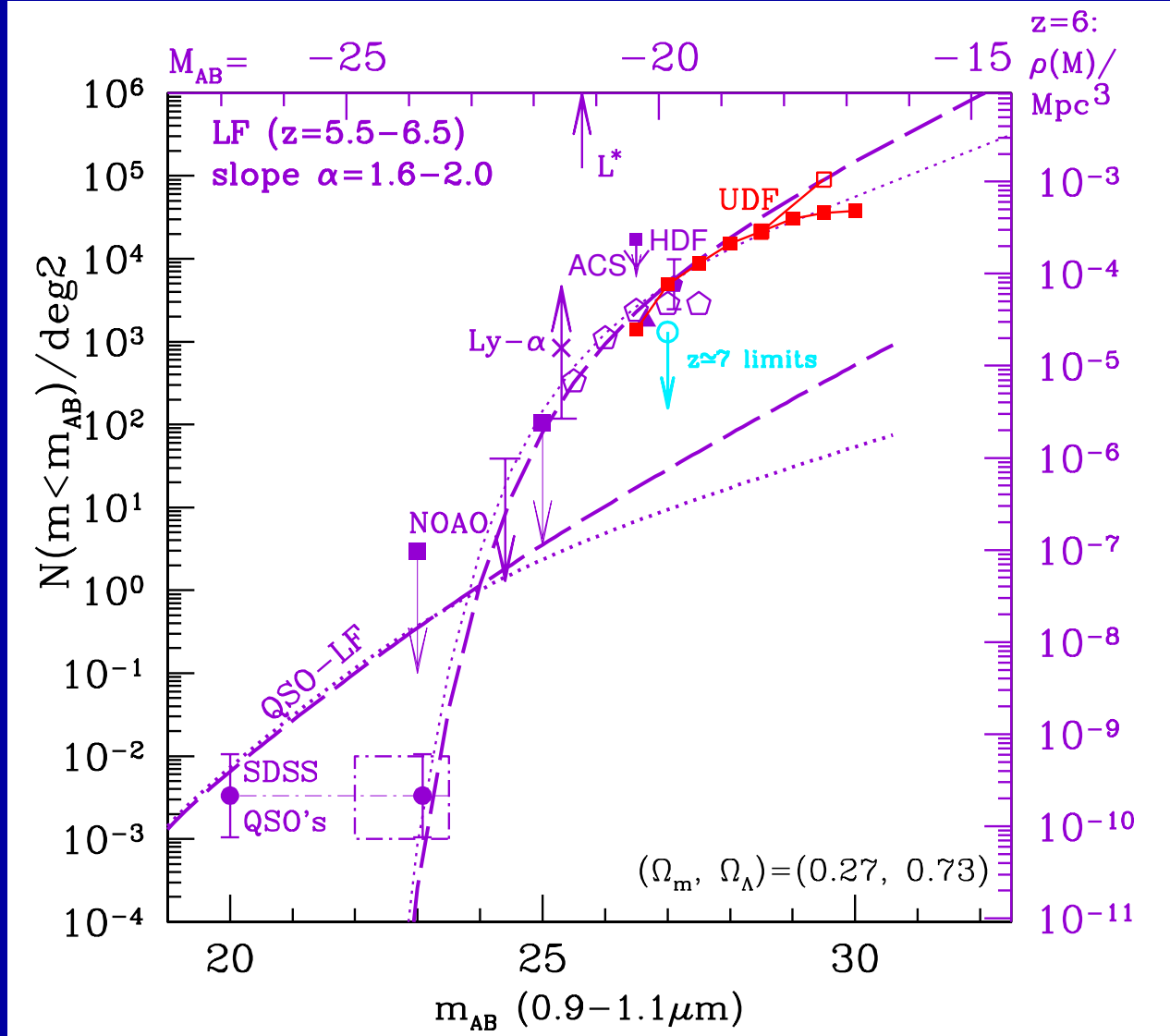
Distant Galaxies in the Hubble Ultra Deep Field
Hubble Space Telescope • Advanced Camera for Surveys

NASA, ESA, R. Windhorst (Arizona State University) and H. Yan (Spitzer Science Center, Caltech)

STScI-PRC04-28

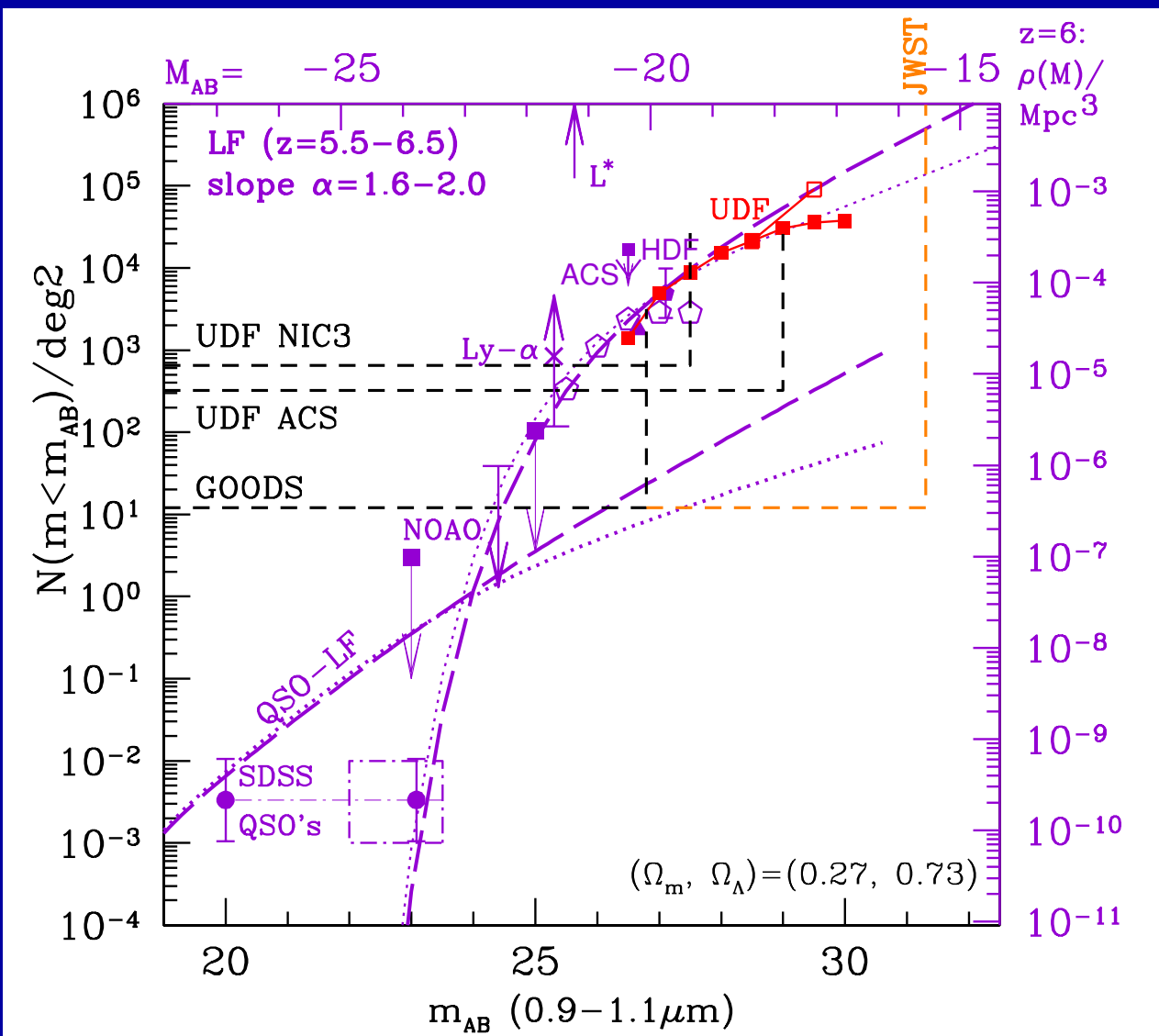
i-band drops in the HUDF: Most are confirmed at $z \approx 6$ (Malhotra et al.)

- (3) How JWST can measure First Light and Reionization

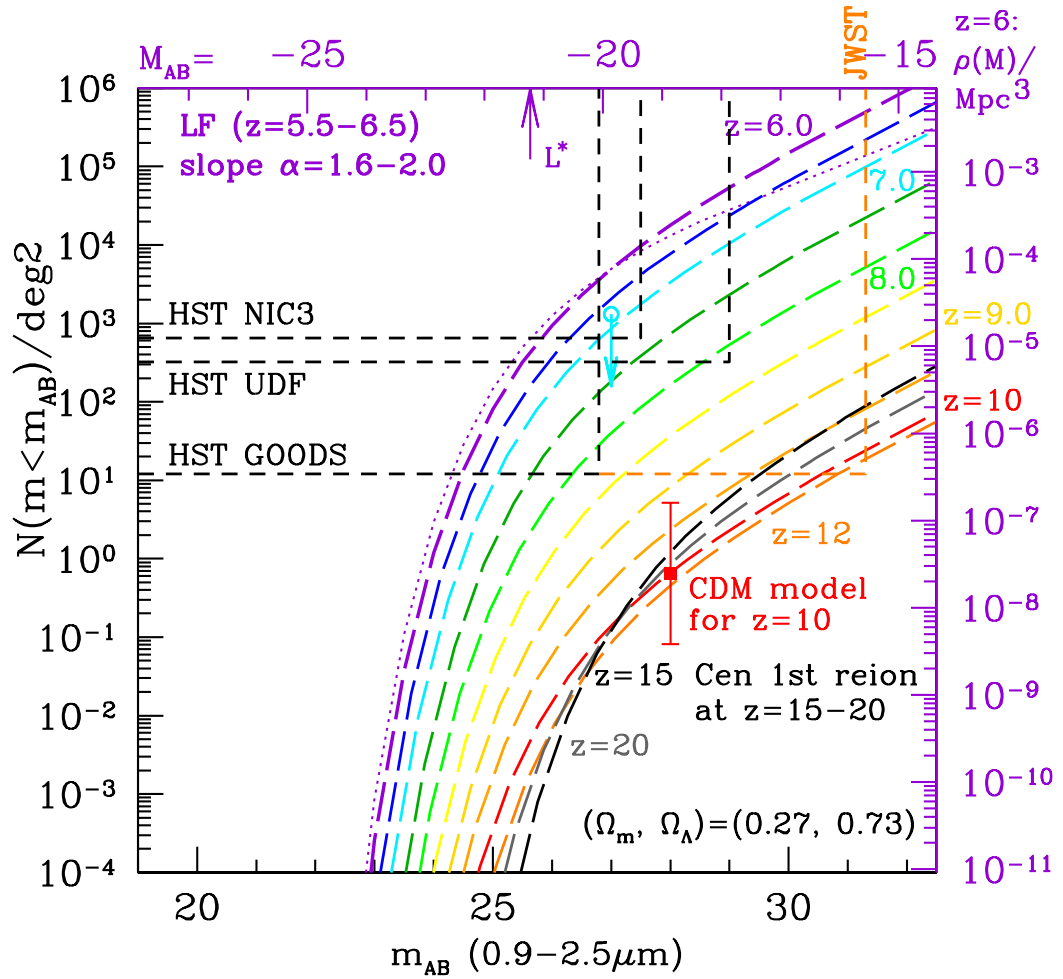


UDF shows that luminosity function of $z \approx 6$ objects (Yan et al. 2004a, b) may be very steep, with faint-end Schechter slope $|\alpha| \approx 1.6-2.0$.

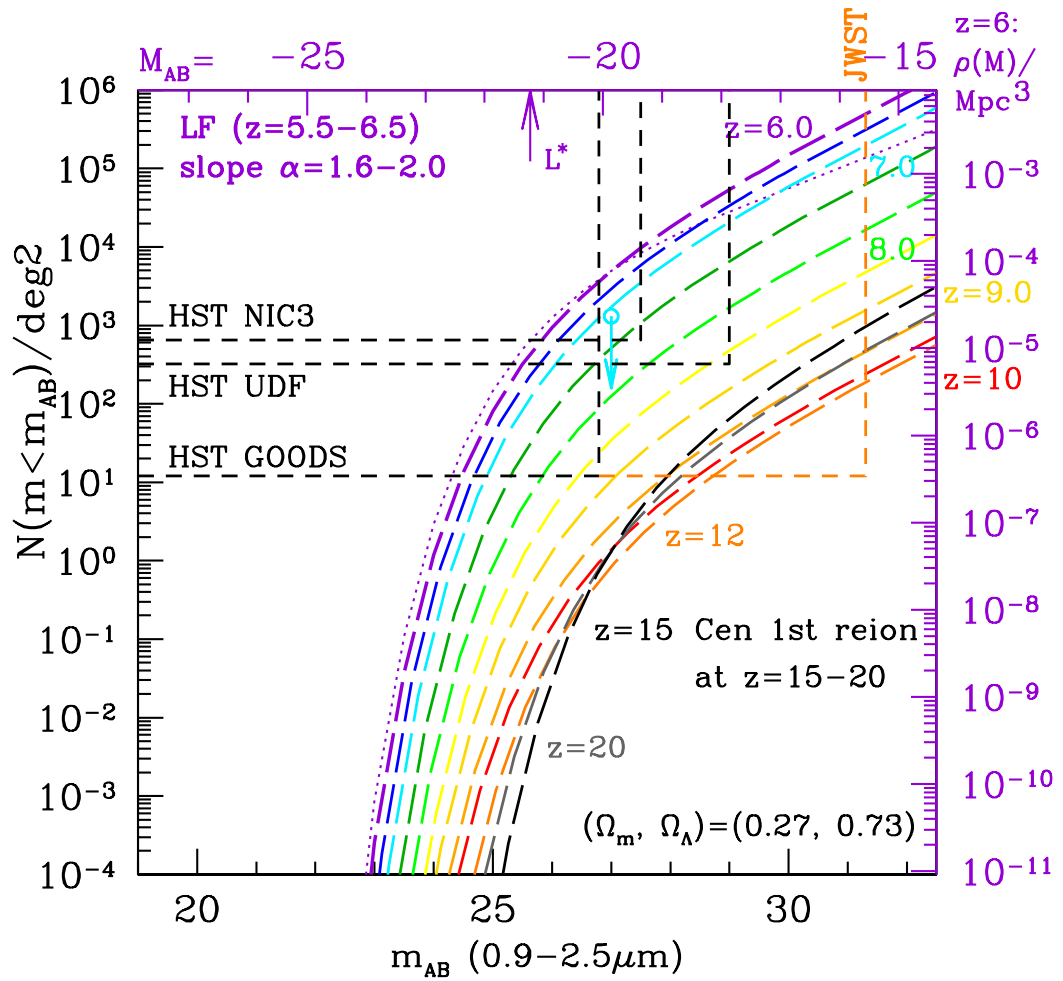
⇒ Dwarf galaxies and not quasars likely completed the reionization epoch at $z \approx 6$. This is what JWST will observe in detail.



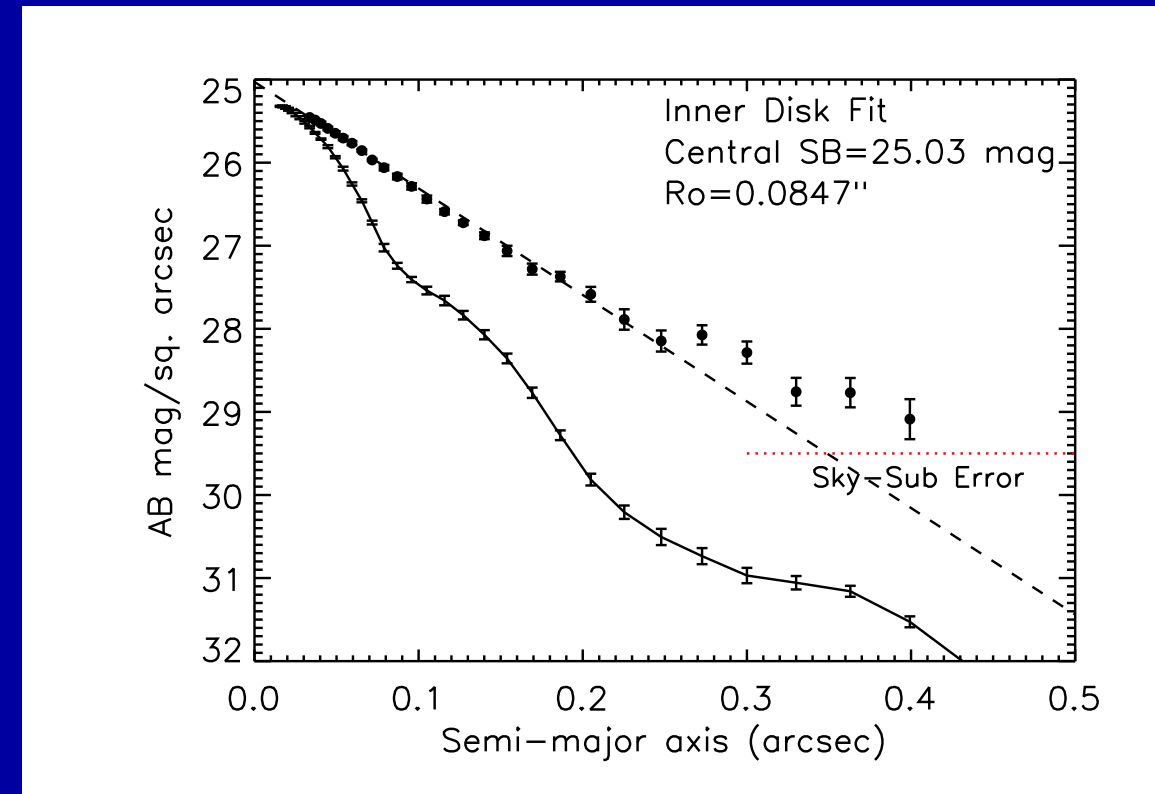
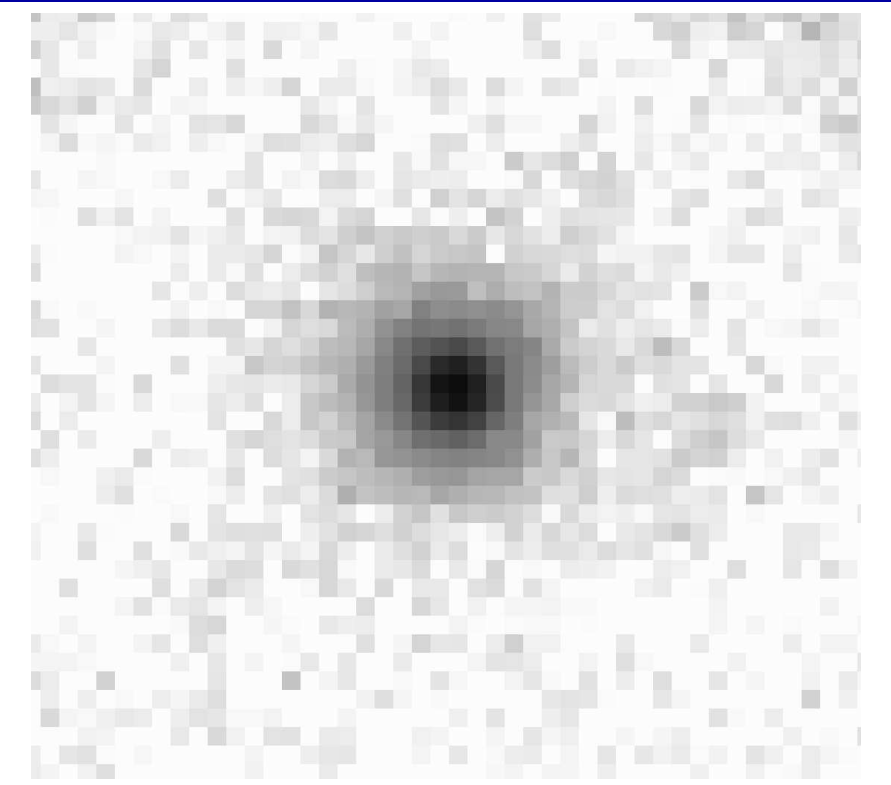
- HST/ACS has made significant progress at $z \approx 6$, surveying very large areas (GOODS, GEMS, COSMOS), or using very long integrations (HUDF). ACS can detect objects at $z \lesssim 6.5$, but its discovery space $A \cdot \Omega \cdot \Delta \log(\lambda)$ cannot map the entire reionization epoch. NICMOS similarly is limited to $z \lesssim 8-10$. JWST will be able to trace the entire reionization epoch.



- With proper survey strategy (area AND depth), JWST can trace the entire reionization epoch, i.e. detect some of the first star-forming objects.
- For this to be successful in realistic or conservative model scenarios, JWST needs the quoted sensitivity/aperture (A), field-of-view ($\text{FOV}=\Omega$), and wavelength range ($0.7\text{-}28\mu\text{m}$).



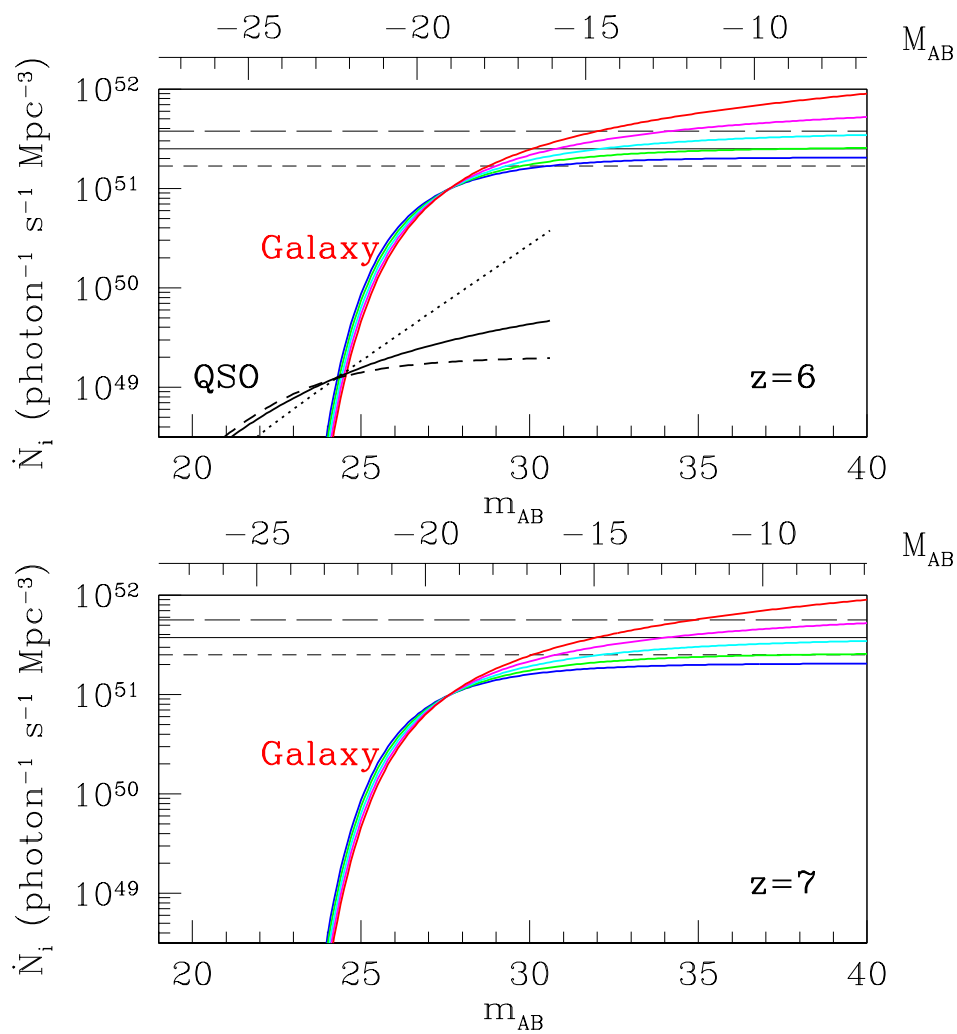
- In more optimistic scenarios, the surface density may be $\gtrsim 10\times$ higher at $z \gtrsim 10$, but JWST design must assume that objects at $z \simeq 20$ are rare, since volume element is small and JWST samples brighter part of LF at $z \gtrsim 10$.



Sum of 49 isolated i-drops:
=5000 hrs HUDF z-band.
[≈ 330 hrs JWST 1 μm]

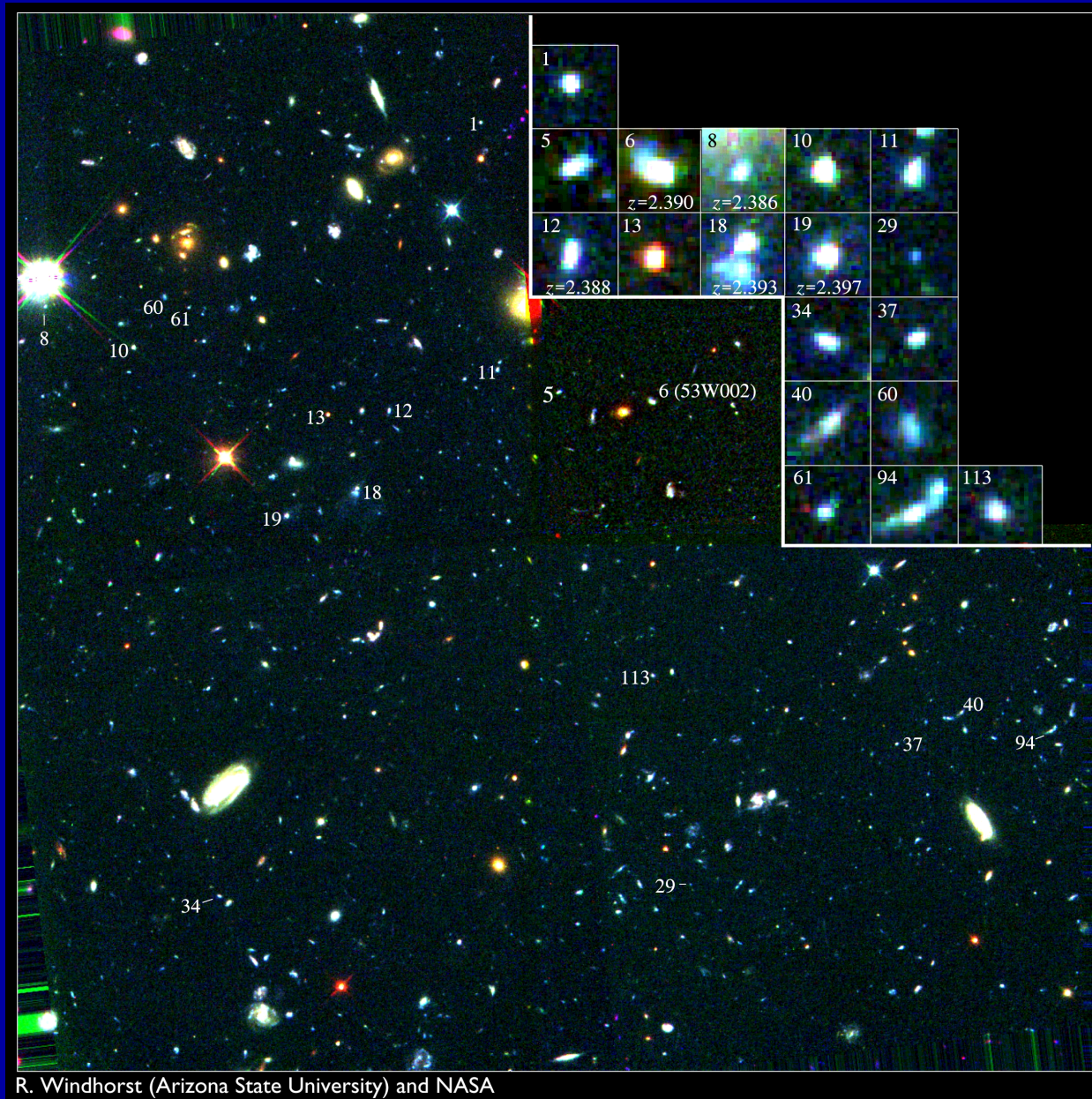
ACS light-profile, PSF and sky-error:
Deviates from exp. disk at $r_e \gtrsim 0.25''$
 \Rightarrow Dyn. age ($z \approx 6$) $\simeq 100$ -200 Myr

HST/ACS cannot accurately measure individual light-profiles at $z \approx 6$.
JWST can do this well for $z \gtrsim 6$ in very long integrations.
Dynamical timescale \simeq SED timescale \Rightarrow Bulk of SF at $z_{form} \approx 7.0 \pm 0.5??$



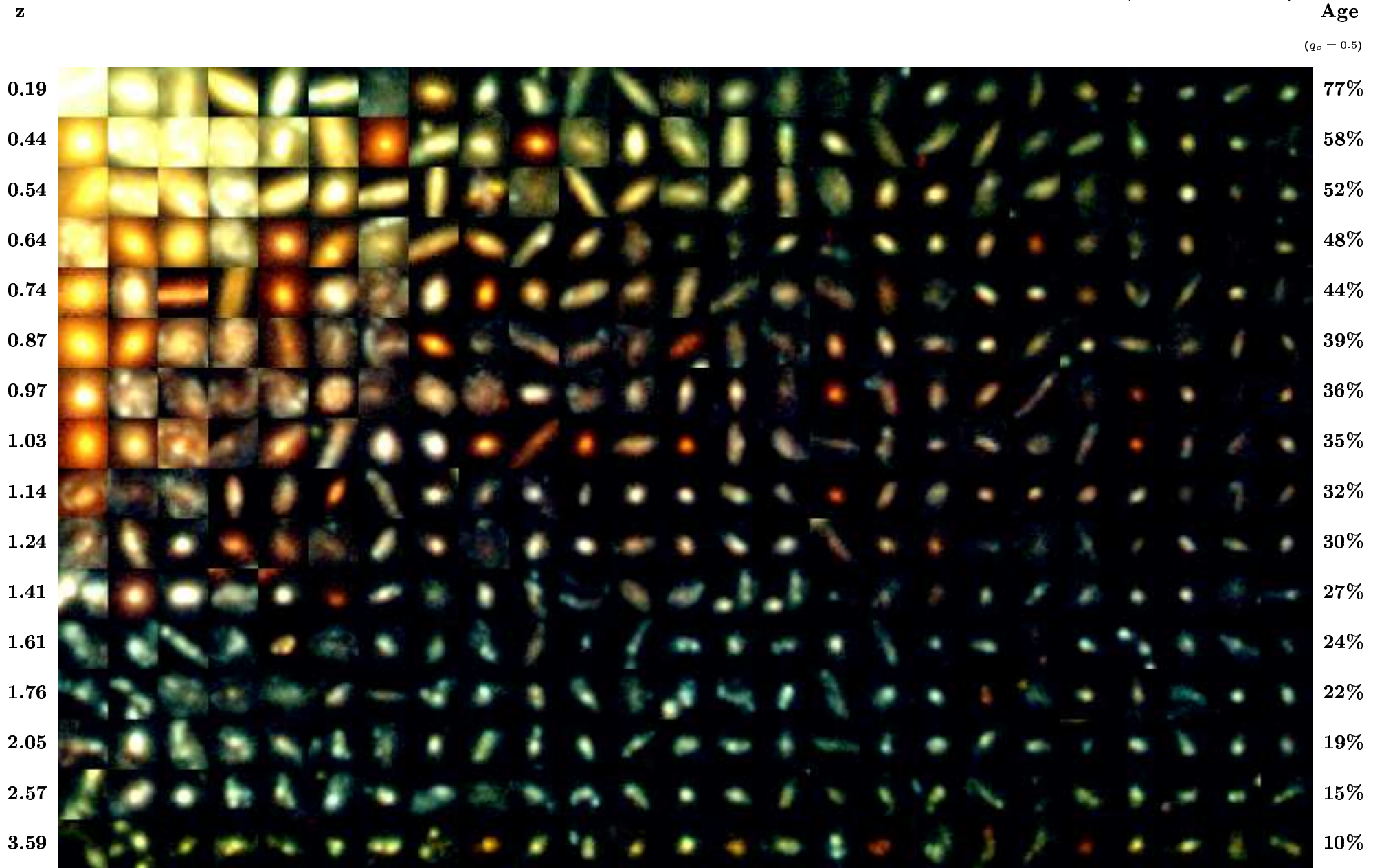
- A steep LF of $z \approx 6$ objects (Yan & Windhorst 2004) could provide enough UV-photons to complete the reionization epoch at $z \approx 6$.
- Pop II dwarf galaxies may not have started shining *pervasively* much before $z \approx 7$ –8, or no H-I would be seen in the foreground of $z \gtrsim 6$ quasars.
- JWST will measure this numerous population of dwarf galaxies from the end of the reionization epoch at $z \approx 6$ into the epoch of First Light (Pop III stars) at $z \gtrsim 10$.

- (4) How JWST can measure Galaxy Assembly

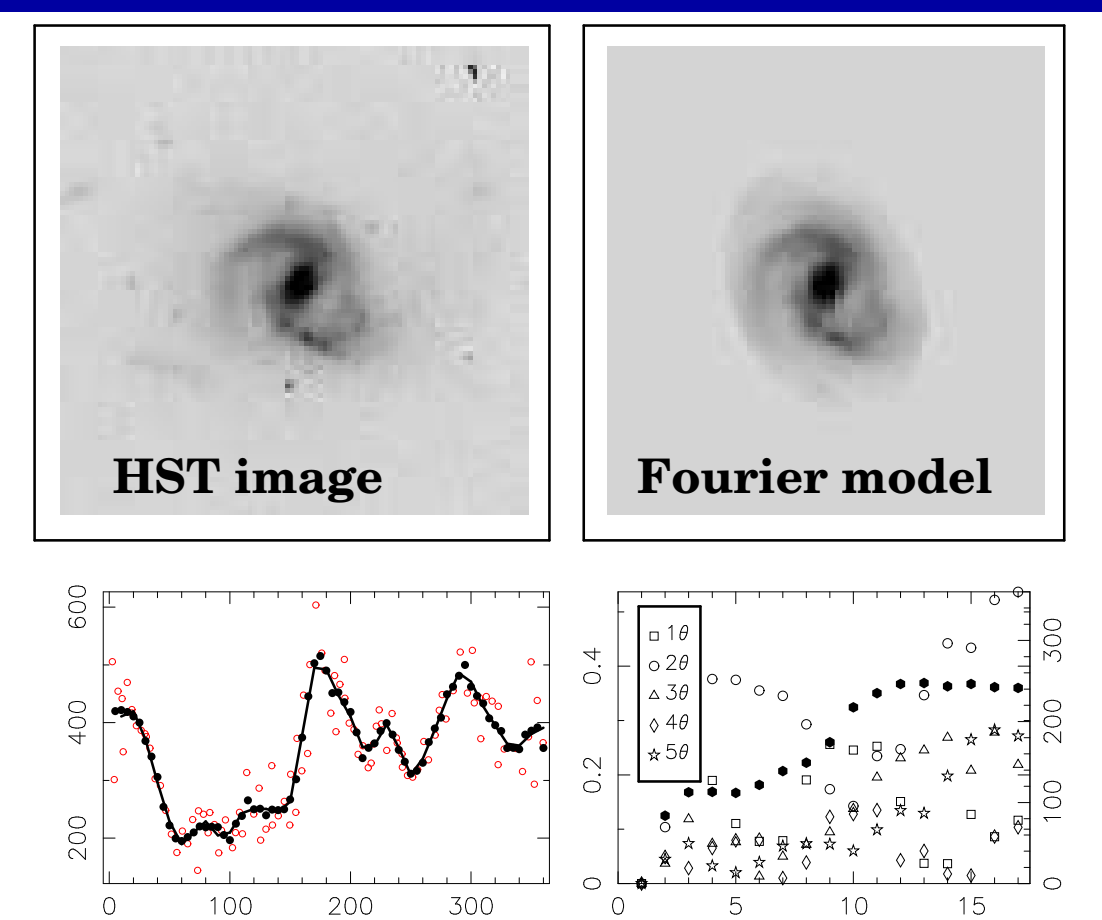


One of the remarkable discoveries of HST was how numerous and small faint galaxies are — the building blocks of the giant galaxies seen today.

THE HUBBLE DEEP FIELD CORE SAMPLE ($I < 26.0$)



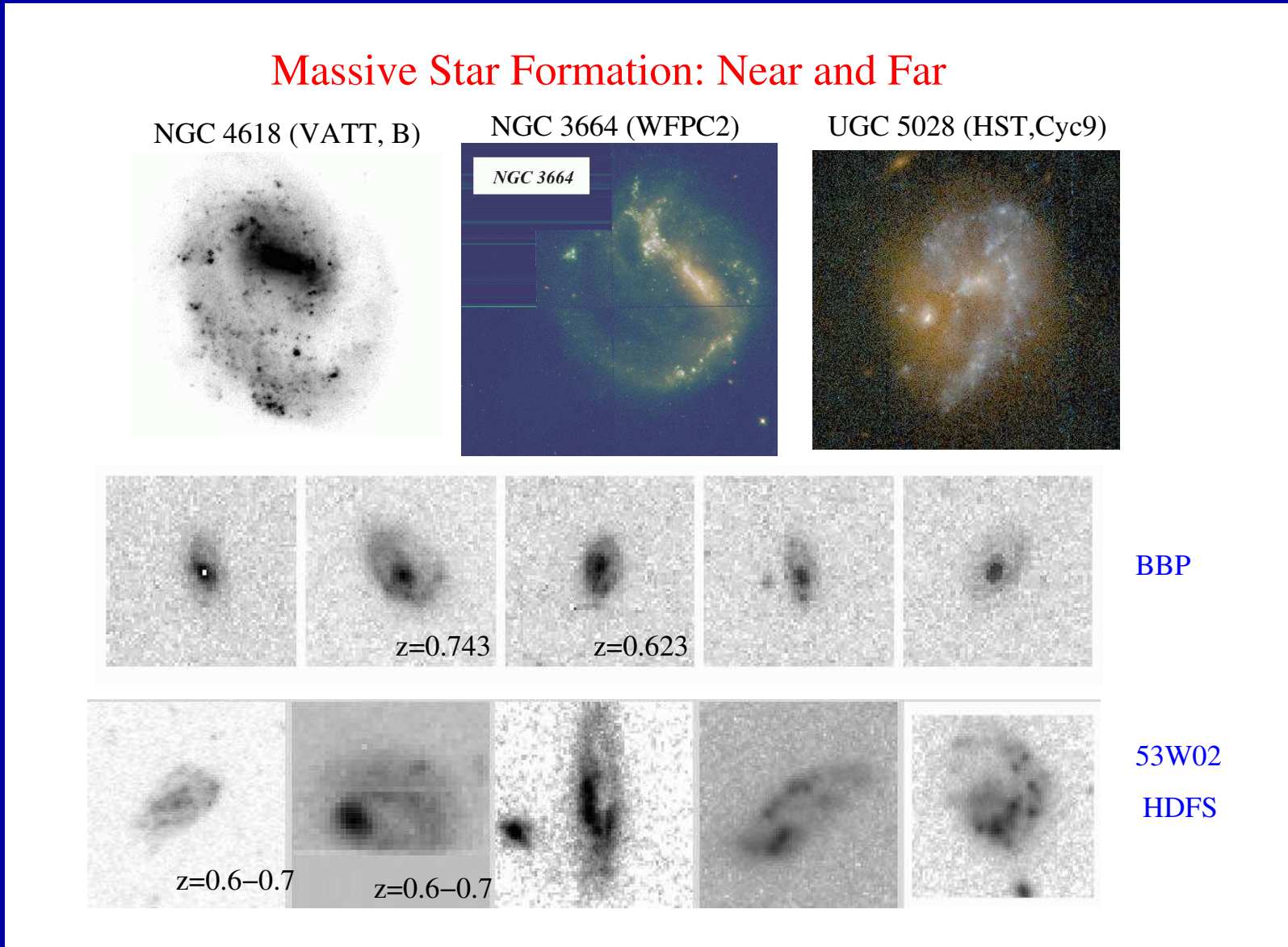
- (4) How JWST can measure Galaxy Assembly
- Galaxies of Hubble types formed over a wide range of cosmic time, but with a notable phase transition around $z \simeq 0.5\text{--}1.0$:
 - (1) Subgalactic units rapidly merge from $z \simeq 7 \rightarrow 1$ to grow bigger units.
 - (2) Merger products start to settle as galaxies with giant bulges or large disks around $z \simeq 1$. These evolved mostly passively since then, resulting in the giant galaxies that we see today.
- JWST can measure how galaxies of all types formed over a wide range of cosmic time, by accurately measuring their distribution over rest-frame structure and type as a function of redshift or cosmic epoch.



Fourier Decomposition is a robust way to measure galaxy morphology and structure in a quantitative way (Odewahn et al. 2002):

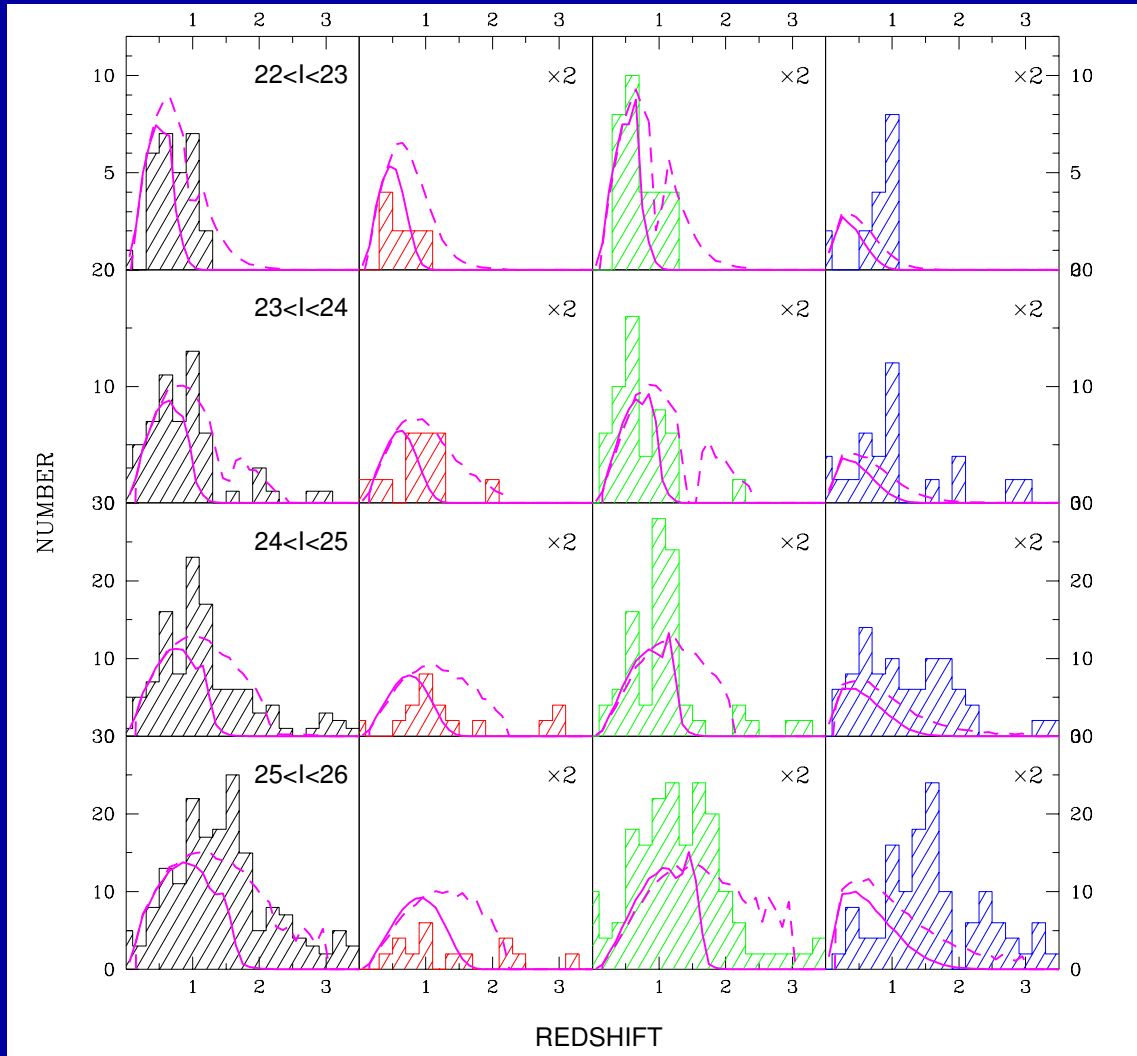
- (1) Fourier series are made in successive concentric annuli.
- (2) Even Fourier components indicate symmetric parts (arms, rings)
- (3) Odd Fourier components indicate asymmetric parts (bars etc).
- (4) JWST can measure the evolution of each feature directly.

Massive Star Formation: Near and Far



Fourier Decomposition of nearby and distant galaxies in JWST images will directly trace the evolution of bars, rings, spiral arms, and other structural features. This measures the detailed history of galaxy assembly in the epoch $z \simeq 1-3$ when most of today's giant galaxies were made.

Total Ell/S0 Sabc Irr/Mergers



- JWST can measure how galaxies of all Hubble types formed over a wide range of cosmic time, by measuring their redshift distribution as a function of rest-frame type.
- For this, the types must be well imaged for large samples from deep, uniform and high quality multi-wavelength images, which JWST can do.

NGC 3310



ESO0418-008



UGC06471-2



Ultraviolet Galaxies

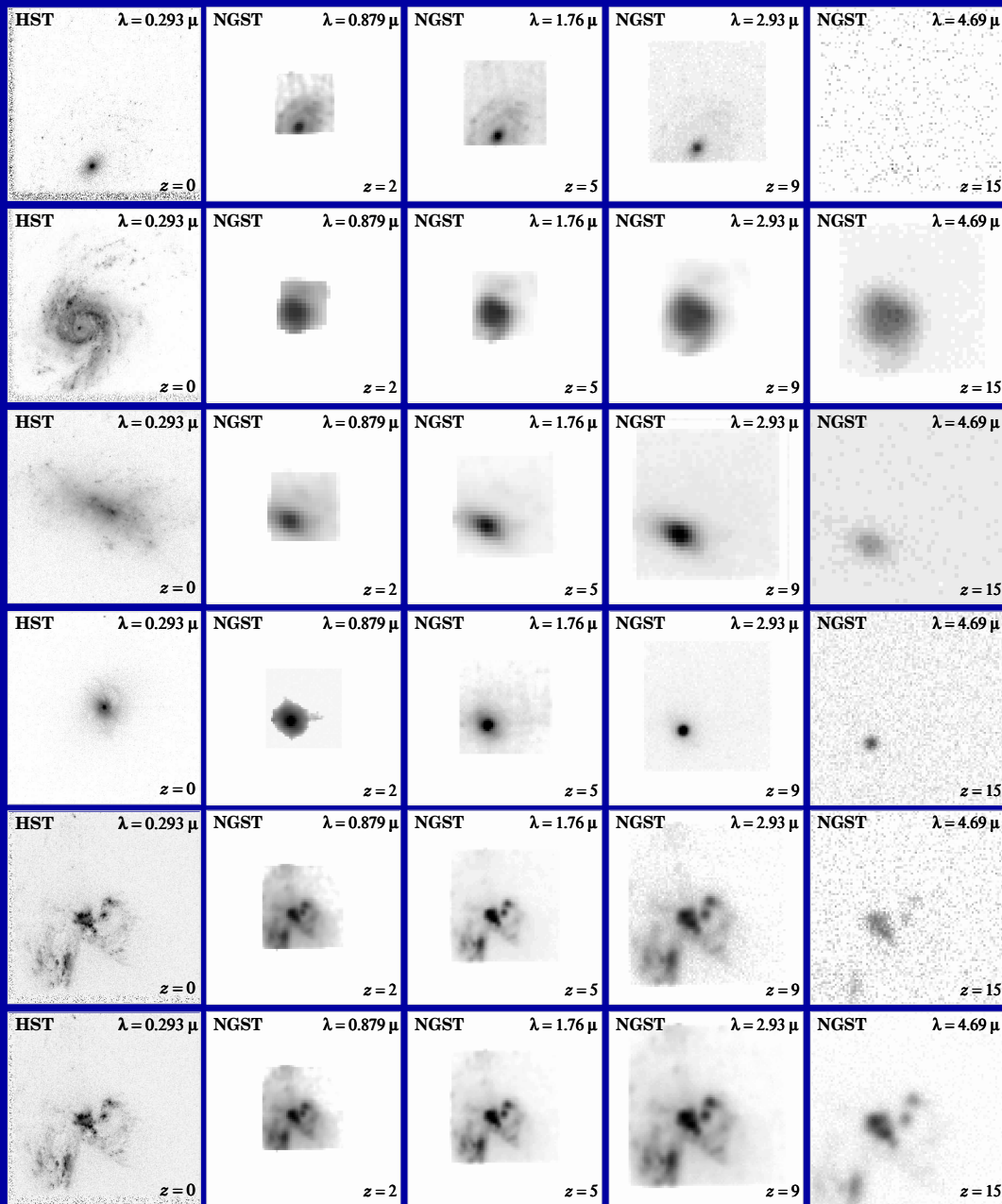
NASA and R. Windhorst (Arizona State University) • STScI-PRC01-04

HST • WFPC2

- The uncertain rest-frame UV-morphology of galaxies is dominated by young and hot stars, with often copious amounts of dust superimposed.
- This makes comparison with very high redshift galaxies seen by JWST complicated, although with good images a quantitative analysis of the restframe-wavelength dependent morphology and structure can be made.

(5) Predicted Galaxy Appearance for JWST at $z \simeq 1-15$

HST $z=0$ JWST $z=2$ $z=5$ $z=9$ $z=15$



With proper restframe-UV training, JWST can quantitatively measure the evolution of galaxy morphology and structure over a wide range of cosmic time:

- (1) Most disks will SB-dim away at high z , but most formed at $z \lesssim z_{form} \simeq 1-2$.
- (2) High SB structures are visible to very high z .
- (3) Point sources (AGN) are visible to very high z .
- (4) High SB-parts of mergers/train-wrecks are visible to very high z .

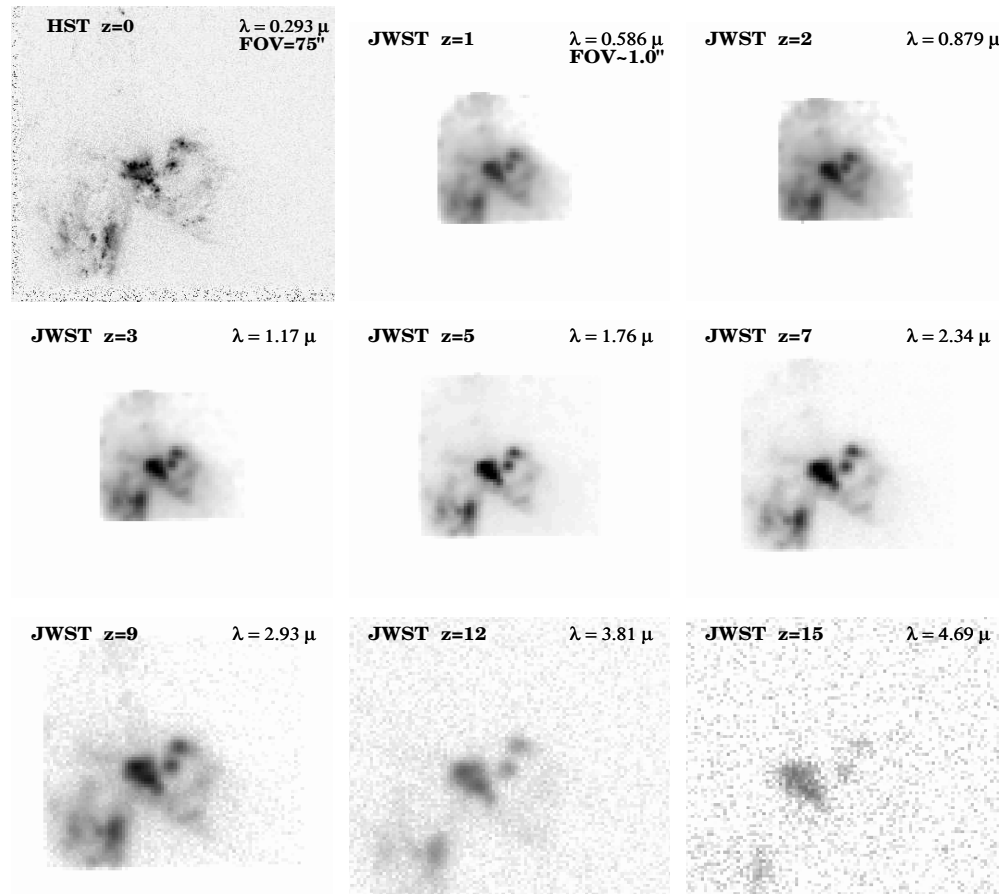


Fig. 4.06.a. JWST simulations based on HST/WFPC2 F300W images of the merger UGC06471-2 ($z=0.0104$). Note that the two unresolved star-bursting knots in the center remain visible until $z\sim 12$, beyond which the SB-dimming also kills their flux. This is the NOMINAL JWST [= (GOALS+REQUIREMENTS)/2].

ASSUMPTIONS: COSMOLOGY: $H_0=71 \text{ km/s/Mpc}$, $\Omega_m=0.27$, and $\Omega_\Lambda=0.73$.

INSTRUMENT: 6.0 m effective aperture, JWST/NIRCam, 0.034 $''/\text{pix}$, $RN=5.0 \text{ e}^-$, $Dark=0.020 \text{ e}^-/\text{sec}$, NEP $H\text{-band Sky}=21.7 \text{ mag/arcsec}^2$ in L2, Zodiacal spectrum, $t_{exp}=1.0 \text{ hrs}$, read-out every 900 sec ("NOMINAL").

Row 1: $z=0.0$ (HST $\lambda=0.293\mu\text{m}$, FWHM=0.04 $''$), $z=1.0$ (JWST $\lambda=0.586\mu\text{m}$, FWHM=0.084 $''$), and $z=2.0$ (JWST $\lambda=0.879\mu\text{m}$, FWHM=0.084 $''$). **Row 2:** $z=3.0$ (JWST $\lambda=1.17\mu\text{m}$, FWHM=0.084 $''$), $z=5.0$ (JWST $\lambda=1.76\mu\text{m}$, FWHM=0.084 $''$), and $z=7.0$ (JWST $\lambda=2.34\mu\text{m}$, FWHM=0.098 $''$). **Row 3:** $z=9.0$ (JWST $\lambda=2.93\mu\text{m}$, FWHM=0.122 $''$), $z=12.0$ (JWST $\lambda=3.81\mu\text{m}$, FWHM=0.160 $''$), and $z=15.0$ (JWST $\lambda=4.69\mu\text{m}$, FWHM=0.197 $''$)

The galaxy merger UGC06471-2 ($z=0.0104$) is a major and very dusty collision of two massive disk galaxies.

It shows two bright unresolved star-bursting knots to the upper-right of the center, which remain visible until $z\simeq 12$, beyond which the cosmic SB-dimming kills their flux. These are more typical for the small star-forming objects expected at $z\simeq 10-15$.

This is the NOMINAL JWST = (GOALS+REQUIREMENTS)/2.

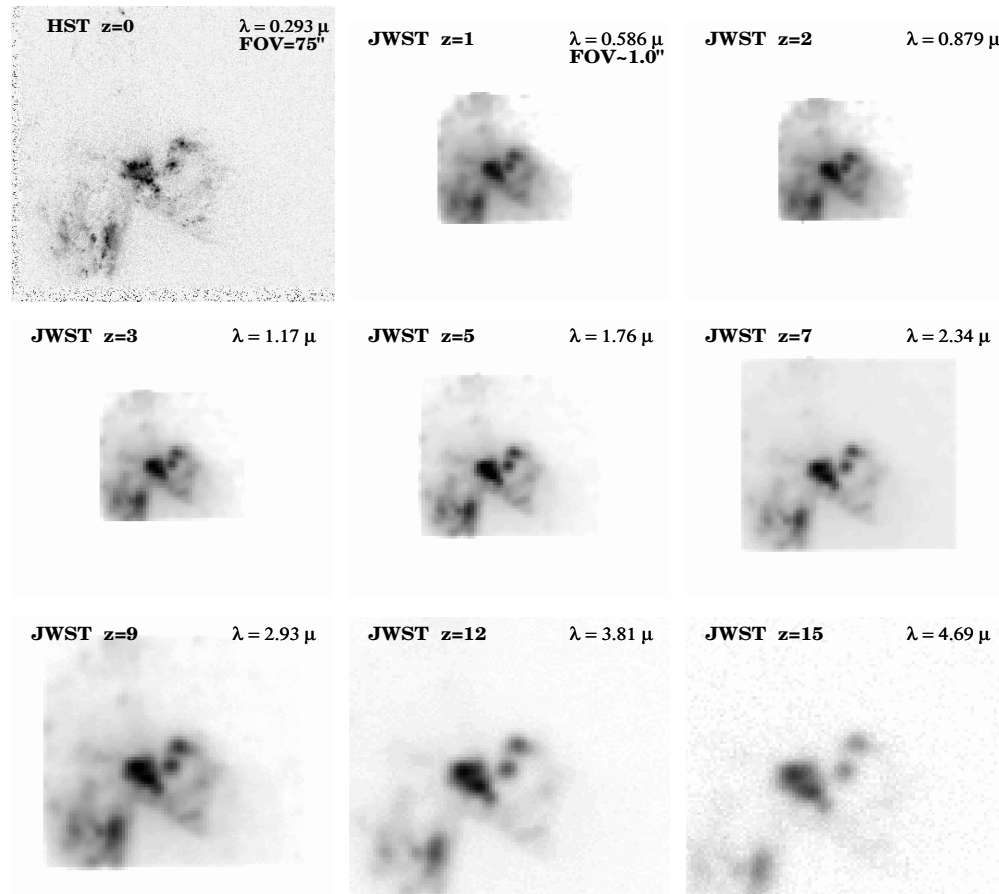


Fig. 4.06.c. JWST simulations based on HST/WFPC2 F300W images of the merger UGC06471-2 ($z=0.0104$). This is the BEST CASE JWST [meeting all GOALS, and $t_{exp}=100$ hrs]. The object is recognizable to $z\simeq 15$.

ASSUMPTIONS: COSMOLOGY: $H_0=71$ km/s/Mpc, $\Omega_m=0.27$, and $\Omega_\Lambda=0.73$.

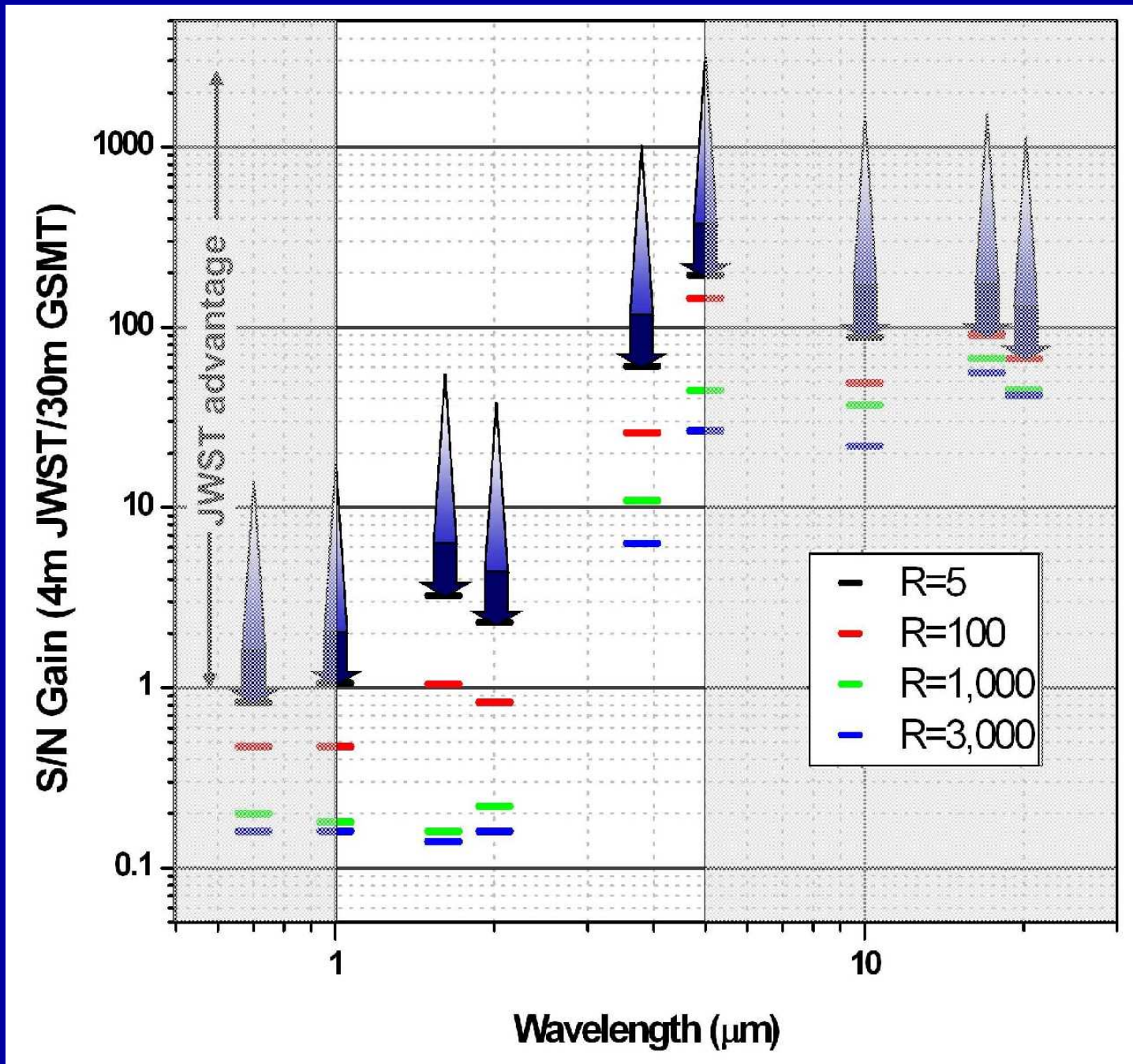
INSTRUMENT: 6.0 m effective aperture, JWST/NIR camera, $0.034''/\text{pix}$, $RN=3.0\text{ e}^-$, $\text{Dark}=0.010\text{ e}^-/\text{sec}$, NEP H-band Sky= 21.7 mag/arcsec^2 in L2, Zodi spectrum, $t_{exp}=100.0\text{ hrs}$, read-out every 900 sec ("GOALS").

Row 1: $z=0.0$ (HST $\lambda=0.293\mu\text{m}$, FWHM= $0.04''$), $z=1.0$ (JWST $\lambda=0.586\mu\text{m}$, FWHM= $0.084''$), and $z=2.0$ (JWST $\lambda=0.879\mu\text{m}$, FWHM= $0.084''$). **Row 2:** $z=3.0$ (JWST $\lambda=1.17\mu\text{m}$, FWHM= $0.084''$), $z=5.0$ (JWST $\lambda=1.76\mu\text{m}$, FWHM= $0.084''$), and $z=7.0$ (JWST $\lambda=2.34\mu\text{m}$, FWHM= $0.098''$). **Row 3:** $z=9.0$ (JWST $\lambda=2.93\mu\text{m}$, FWHM= $0.122''$), $z=12.0$ (JWST $\lambda=3.81\mu\text{m}$, FWHM= $0.160''$), and $z=15.0$ (JWST $\lambda=4.69\mu\text{m}$, FWHM= $0.197''$)

The galaxy merger UGC06471-2 ($z=0.0104$).

This is the BEST CASE JWST. It assumes that all GOALS are met, and that $t_{exp}=100$ hrs. The whole object (including the two star-forming knots) is recognizable to $z\simeq 15$.

This does not imply that observing galaxies at $z=15$ with JWST will be easy. On the contrary, since galaxies formed through hierarchical merging, many objects at $z\simeq 10-15$ will be $10^1-10^4\times$ less luminous, requiring to push JWST to its limits.



Conclusion: JWST must not be descoped to a 4 meter! Arrows indicate:
Top: 6m JWST/Keck; Middle: 6m JWST/30m gb; Bottom: 4m JWST/30m gb

SPARE CHARTS

- References and other sources of material shown:

<http://www.jwst.nasa.gov/>

<http://www.stsci.edu/jwst/>

<http://www.jwst.nasa.gov/ISIM/index.html>

<http://ircamera.as.arizona.edu/nircam/>

<http://ircamera.as.arizona.edu/MIRI/>

<http://www.stsci.edu/jwst/instruments/nirspec/>

<http://www.stsci.edu/jwst/instruments/nirspec/mems.html>

<http://www.stsci.edu/jwst/instruments/guider/>

Gardner, J., Mather, J., Clampin, M., Greenhouse, M., Hammel, H., Hutchings, J., Jakobsen, P., Lilly, S., Lunine, J., McCaughean, M., Mountain, M., Rieke, G., Rieke, M., Smith, E., Stiavelli, M., Stockman, H., Windhorst, R., & Wright, G. (“the JWST Flight Science Working Group”) 2004, Proc. SPIE, Vol. 4014, p. 001–012, in press “The Science Requirements of the James Webb Space Telescope” (and references therein).

Mather, J., Stockman, H. 2000, Proc. SPIE Vol. 4013, p. 2-16, in “UV, Optical, and IR Space Telescopes and Instruments”, Eds. J. B. Breckinridge & P. Jakobsen (Berlin: Springer)



- (1) How will the JWST be automatically deployed?

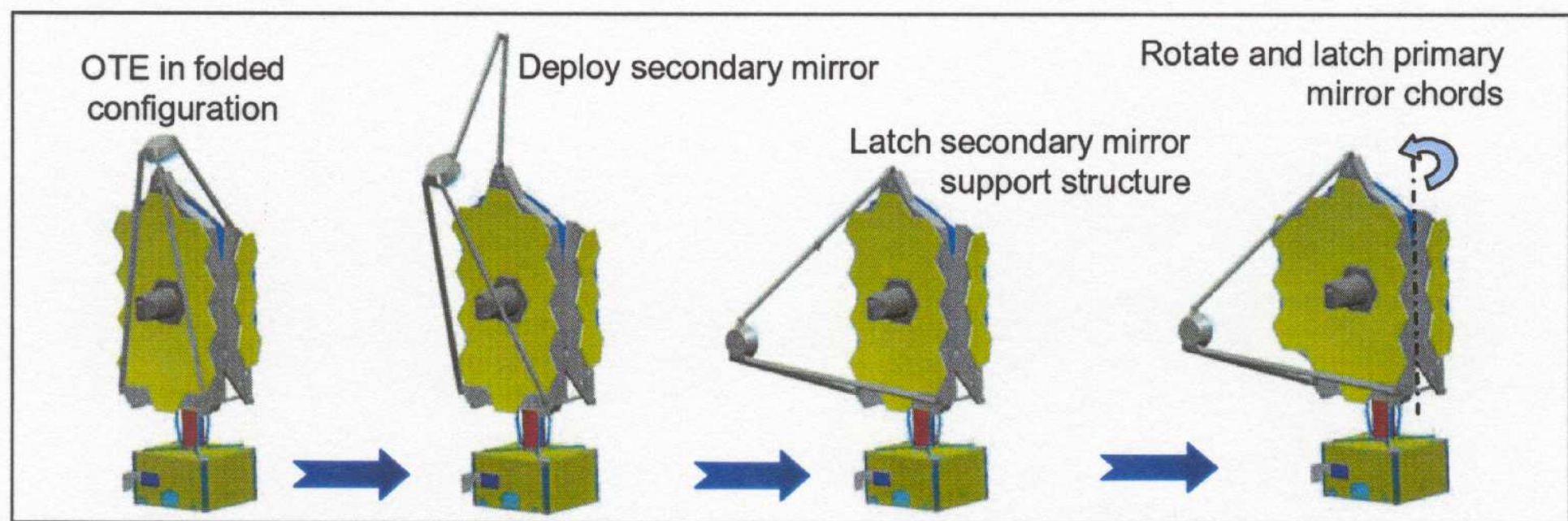


Figure 53. Telescope Deployment Sequence (Deployment steps 4 and 5)

During its several month journey to L2 (shown on a previous page), JWST will be automatically deployed in phases (as shown here), its instruments will be tested, and it will then be inserted into an L2 halo orbit.

From an orbit around the the Earth–Sun Lagrange point L2, JWST can cover the whole sky in segments, have an observing efficiency $\gtrsim 70\%$, and send data back to Earth every day.

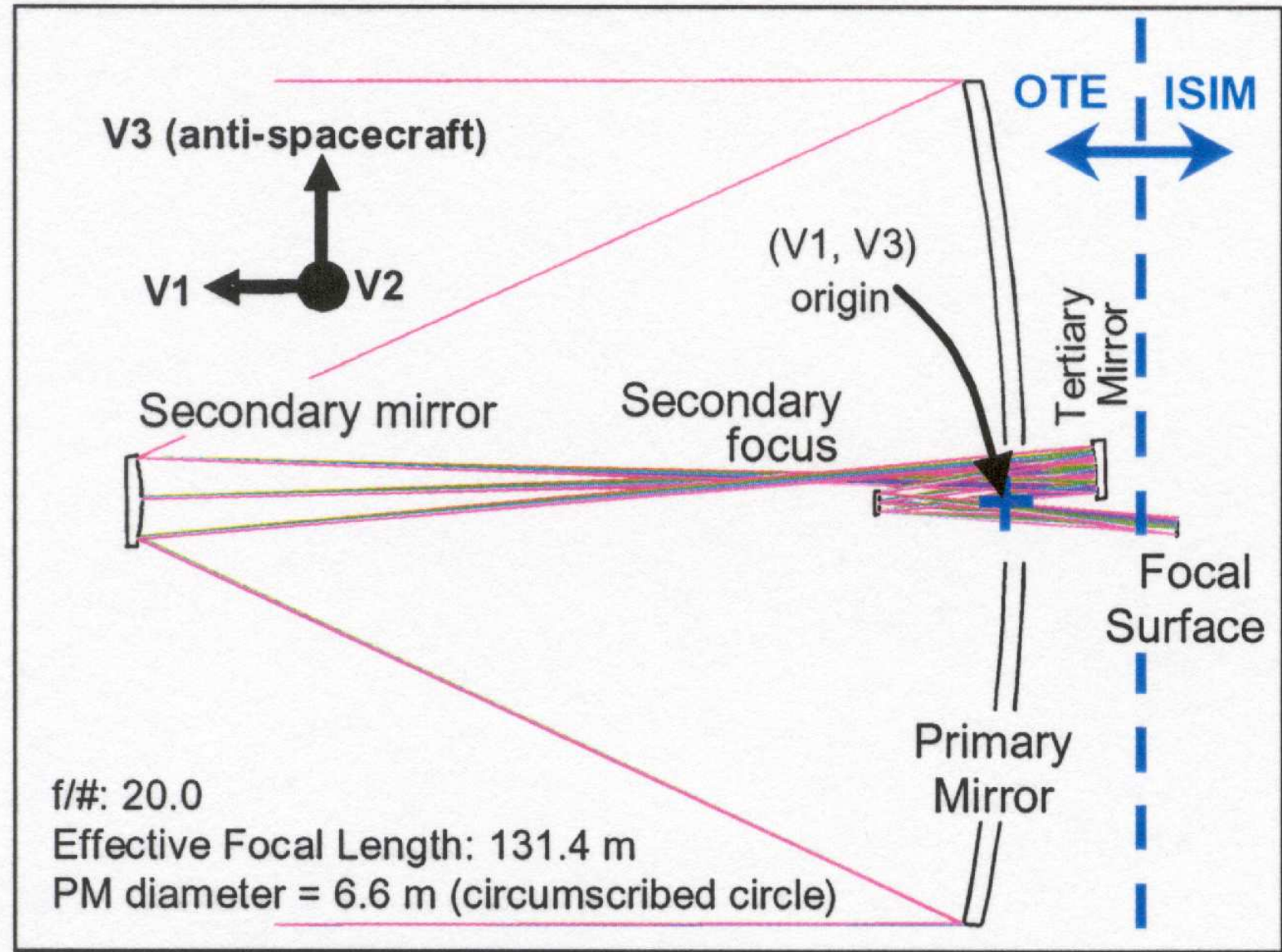
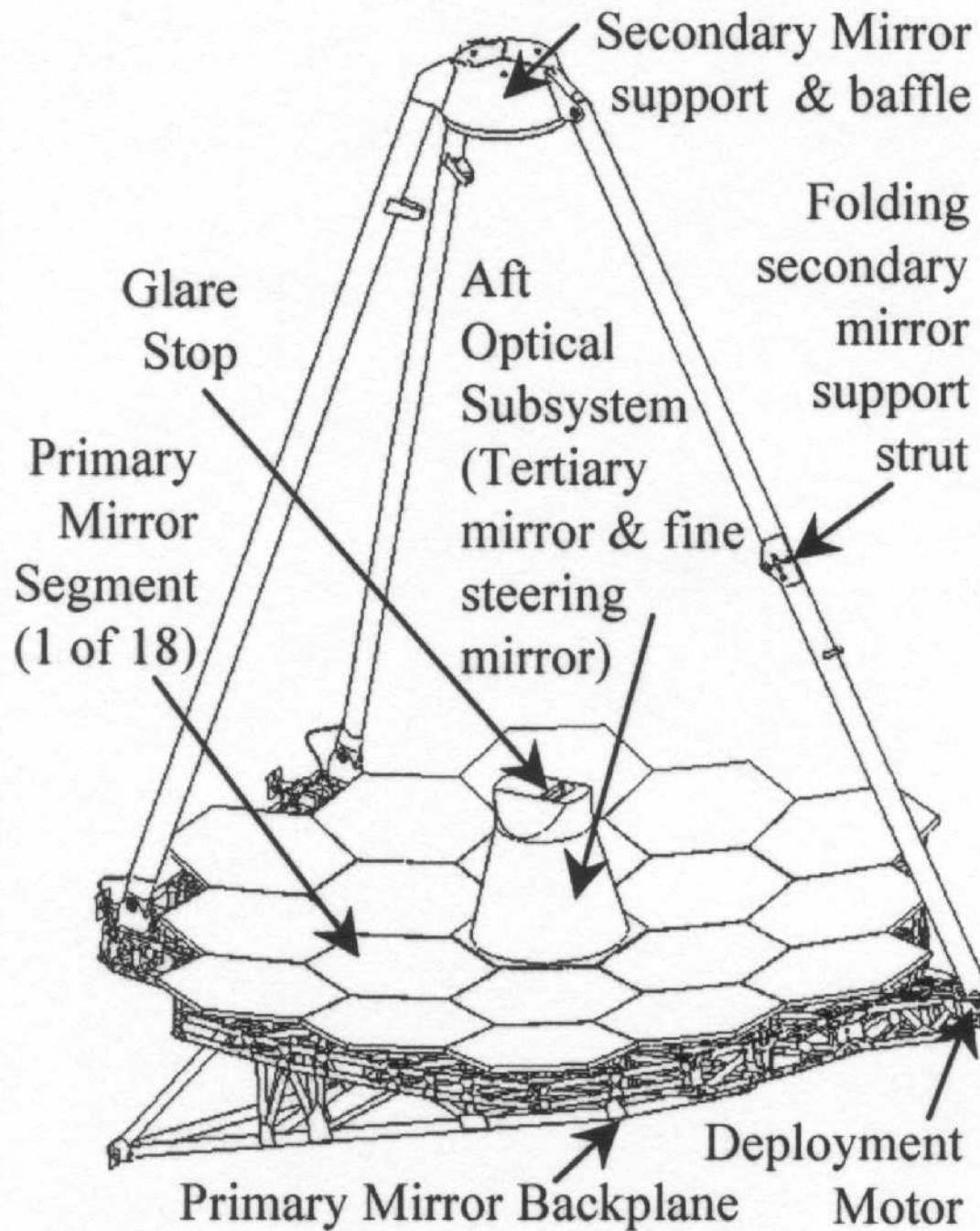
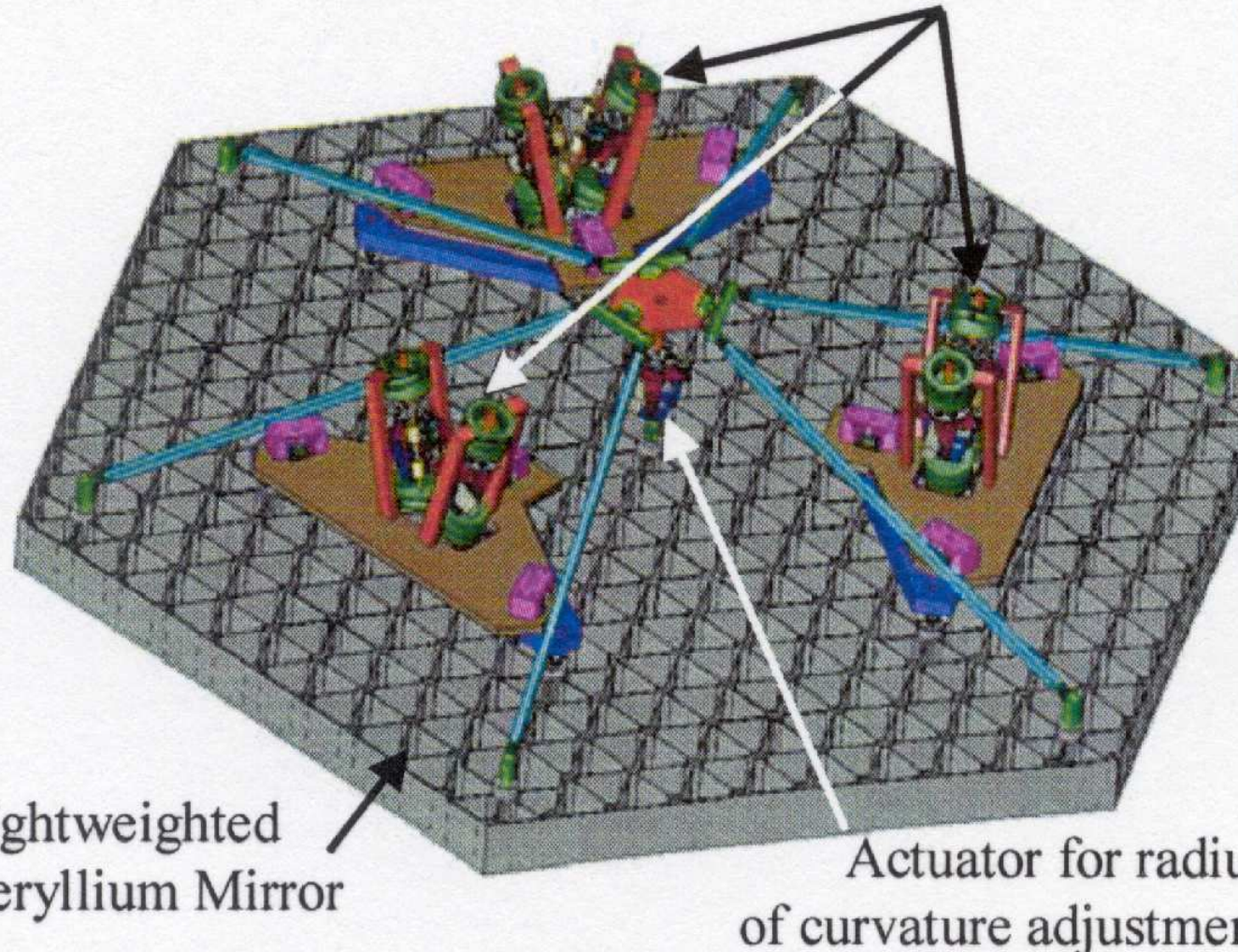


Figure 33. OTE optical layout



Actuators for 6 degrees of freedom rigid body motion



Actuator
development
unit

Figure 36. Rear view of a primary mirror segment.

Table 10. Predicted Performance of the JWST Observatory

| Parameter | Capability |
|-------------------------------------------|--------------------------------------------------------------------------------------------------------------------------------------------------|
| Wavelength | 0.6 to 29 μm . Reflective gold coatings |
| Sensitivity | SNR=10, integration time = τ_i , R= $\lambda/\Delta \lambda$ and Zodiacal of 1.2 times that at north ecliptic pole |
| NIRCam | 12 nJy (1.1 μm , $\tau_i=10,000\text{s}$, and $\lambda/\Delta \lambda = 4$) |
| NIRCam | 10.4 nJy (2.0 μm , $\tau_i=10,000\text{s}$, and $\lambda/\Delta \lambda = 4$) |
| TFI | 368 nJy (3.5 μm , $\tau_i=10,000\text{s}$, and $\lambda/\Delta \lambda = 100$) |
| NIRSpec | 120 nJy (3.0 μm , $\tau_i=10,000\text{s}$, and $\lambda/\Delta \lambda = 100$) |
| NIRSpec | 560 nJy (10 μm , $\tau_i=10,000\text{s}$, and $\lambda/\Delta \lambda = 5$) |
| MIRI | 5000 nJy (21 μm , $\tau_i=10,000\text{s}$, and $\lambda/\Delta \lambda = 4.2$) |
| NIRSpec Med | $5.2 \times 10^{-22} \text{ W m}^{-2}$ (2 μm , $\tau_i=100,000\text{s}$, R= 1000) |
| MIRI Spec | $3.4 \times 10^{-21} \text{ W m}^{-2}$ (9.2 μm , $\tau_i=10,000\text{s}$, R= 2400) |
| MIRI Spec | $3.1 \times 10^{-20} \text{ W m}^{-2}$ (22.5 μm , $\tau_i=10,000\text{s}$, R= 1200) |
| Spatial Resolution & Stability | Encircled Energy of 75% at 1 μm for 150mas radius Strehl ratio of ~ 0.86 at 2 μm . PSF stability better than 1% |

- (2) What instruments will JWST have?

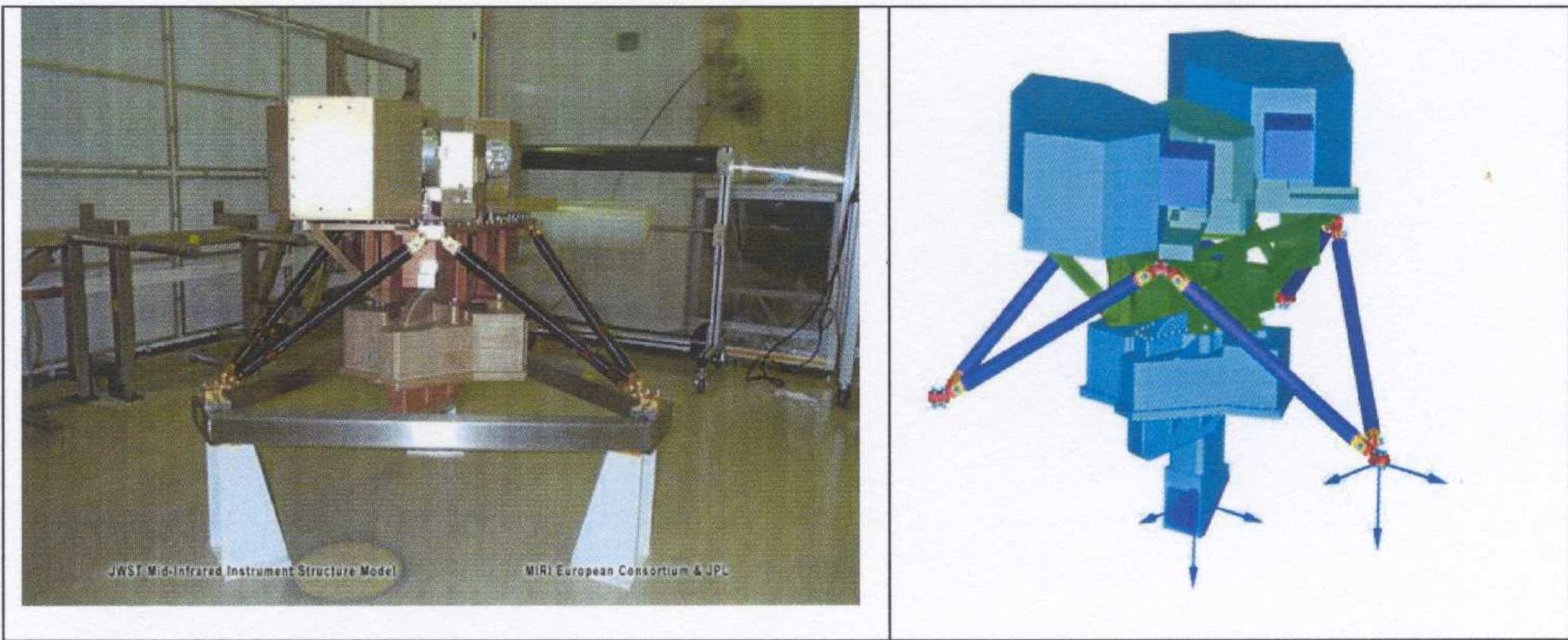


Figure 47. The MIRI structural and thermal model (left) compared to a computer design of the instrument (right).

The Mid-Infra-Red Instrument MIRI made by an UofA + JPL + ESA consortium will do imaging and spectroscopy from 5–28 μm . MIRI is actively cooled by a cryocooler, so that its expected lifetime is at least 5 years.

- (2) What instruments will JWST have?

The Near-Infrared Camera NIRCam made by an UofA + Lockheed + CSA consortium will do imaging from $0.6\text{--}5.3\ \mu\text{m}$ using a suite of broad-, medium-, and narrow-band filters. NIRCam uses two identical and independently operated imaging modules, with two wavelengths observable simultaneously via a dichroic that splits the beam around $2.35\ \mu\text{m}$. Each of these two channels has an independently operated $2!2\times4!6$ FOV. Both channels are Nyquist-sampled: the short-wavelength channel at $2\ \mu\text{m}$ with $0!0317/\text{pixel}$, and the long-wavelength at $4\ \mu\text{m}$ with $0!0648/\text{pixel}$. NIRCam's 10 $2\text{k}\times2\text{k}$ HgCdTe arrays will be passively cooled.

The Near-Infrared Spectrograph NIRSpec made by an ESA + GSFC consortium will do spectroscopy with resolving powers of $R\sim100$ in prism mode, of $R\sim1000$ in multi-object mode using a micro-electromechanical array system (MEMS) of micro-shutters that can open slitlets on previously imaged known objects, and of $R\sim3000$ using long-slit spectroscopy. All NIRSpec spectroscopic modes have a $\sim3.4\times3.4'$ FOV.

- (2) What instruments will JWST have?

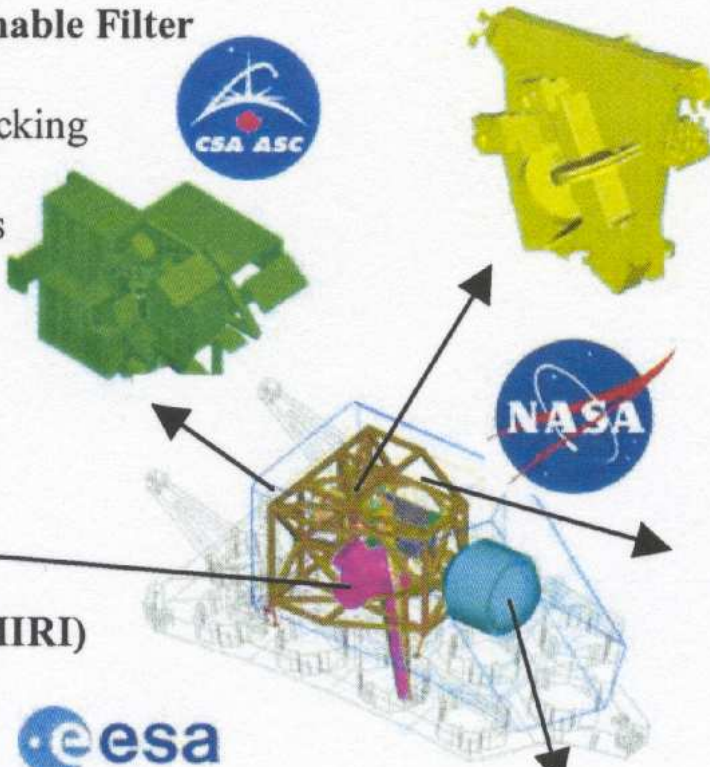
The Mid-Infra-Red Instrument MIRI made by an UofA + JPL + ESA consortium will do imaging and spectroscopy from 5–28 μm . MIRI is actively cooled by a cryocooler and its expected lifetime is at least 5 years.

The Fine Guidance Sensor (FGS) is made by CSA and provide stable pointing at the milli-arcsecond level. The FGS will have sufficient sensitivity and a large enough FOV to find guide stars with $\gtrsim 95\%$ probability at any point in the sky. The FGS will have three simultaneously imaged fields of view of $2.3 \times 2.3'$, one of which feeds a pure guider channel, one feeding a guider channel plus a long-wavelength $R \sim 100$ tunable filter channel with light split by a dichroic, and another feeding the short wavelength tunable filter $R \sim 100$ channel.

JWST has fully redundant imaging and spectroscopic modes. It will not be serviced at L2, and therefore will undergo an extensive series of ground-testing and thermal vacuum testing in 2008–2009, after its main construction in 2004–2008. The main NASA contractor is Northrop Grumman Space Technology (“NGST”) in Redondo Beach (CA).

Fine Guidance Sensor & Tunable Filter

- 0.6 to 5 μm operation
 - Guide star acquisition & tracking
 - Tunable filter imager
- 2 (2048x2048) 68mas pixels



Mid Infrared Instrument (MIRI)

- 5 to 28 μm operation
 - Science Discovery Space
 - Imaging
- 1 (1024x1024) 110mas pixels
- Spectroscopy
- 2 (1024x1024) 200-470mas pixels



Near Infrared Camera (NIRCam)

- 0.6 to 5 μm operation
- Coronagraph imaging capability
- Supports WFS&C
- 2 (4096x4096) 31mas pixels
- 2 (2048x2048) 62mas pixels



Near Infrared Spectrometer (NIRSpec)

- 0.6 to 5 μm operation
- Simultaneous Spectra of > 100 objects
- $\lambda/\Delta\lambda \sim 100$ to 1000
- 2 (2048x2048) 100mas pixels



Solid Hydrogen Dewar

- Cools MIRI detectors to ~7K
- 5 year lifetime

Figure 37. ISIM element and its science instrumentation.

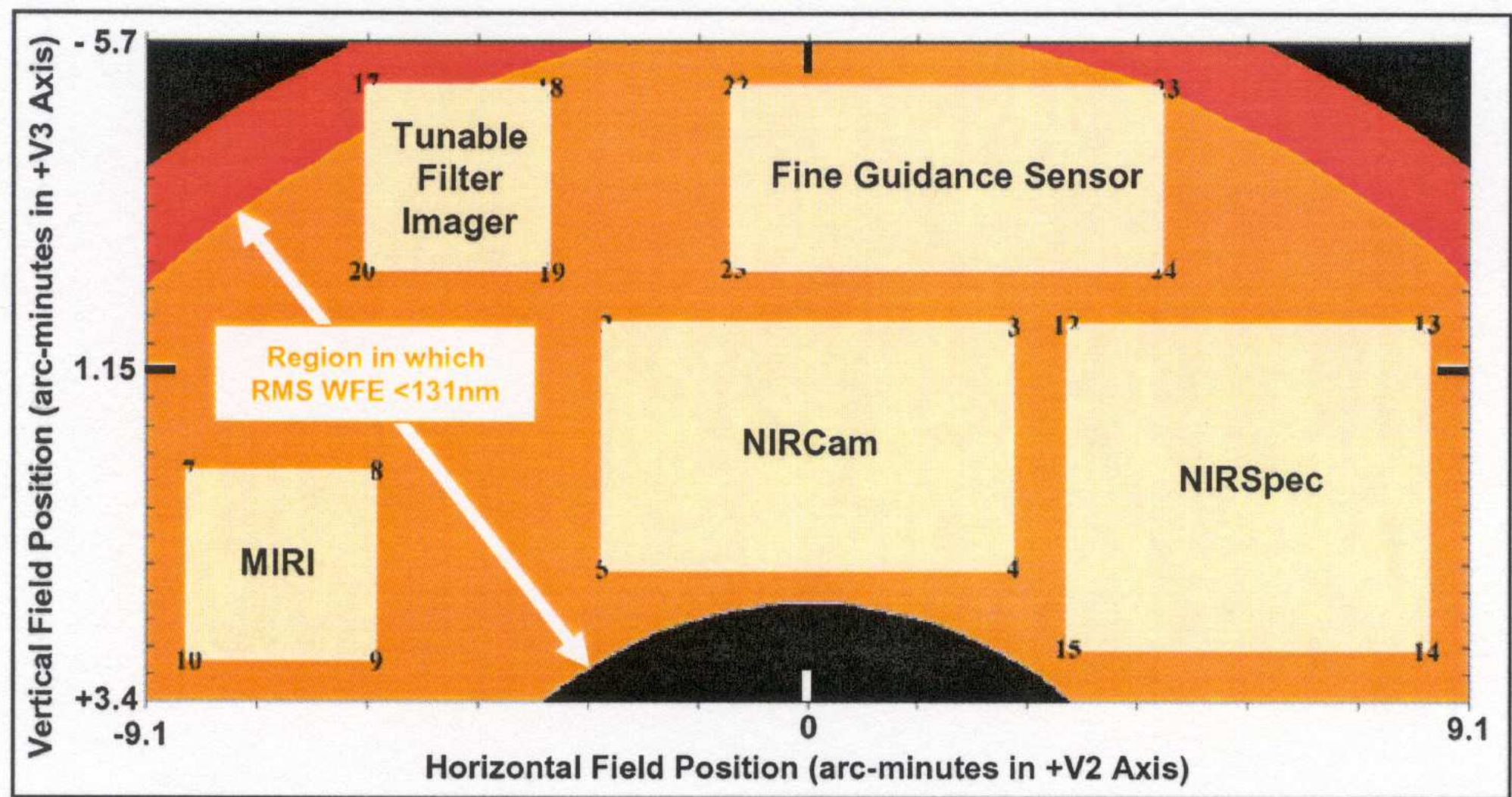


Figure 34. Placement of the ISIM instrument FPAs in the OTE field of view.

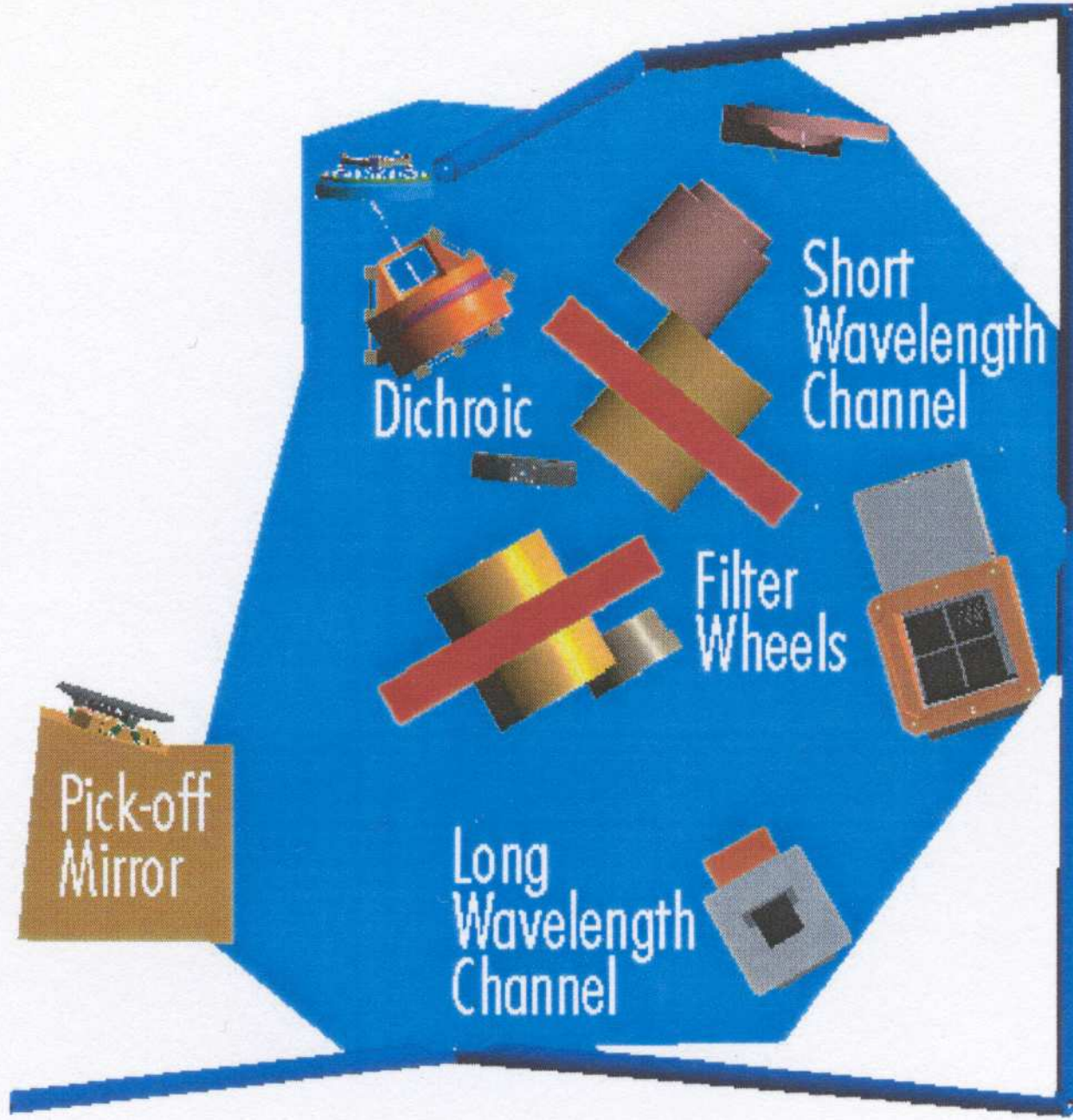


Figure 43. Optical layout of one of two NIRCam imaging modules.

MIRI IFUs fields of view

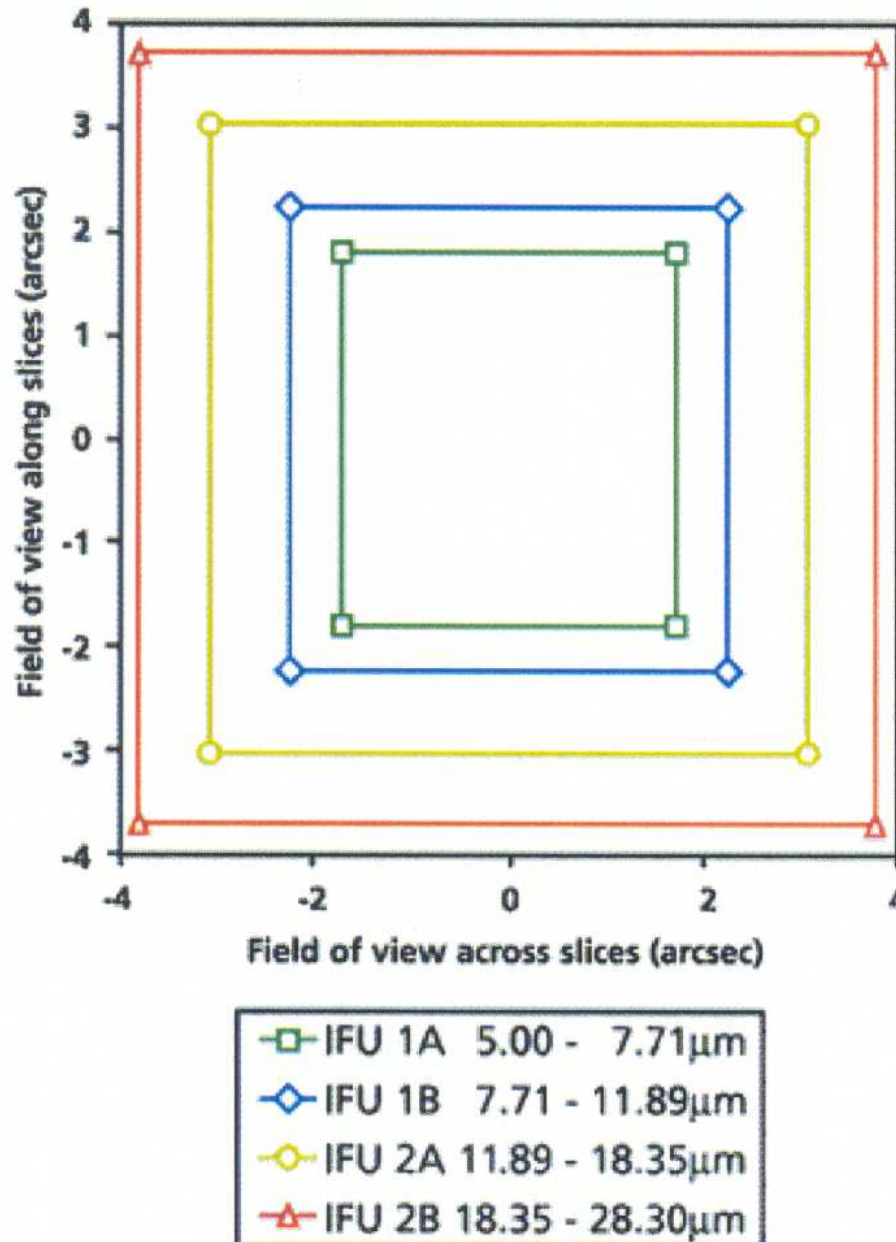


Figure 49. Fields of view of the MIRI IFU spectrograph.

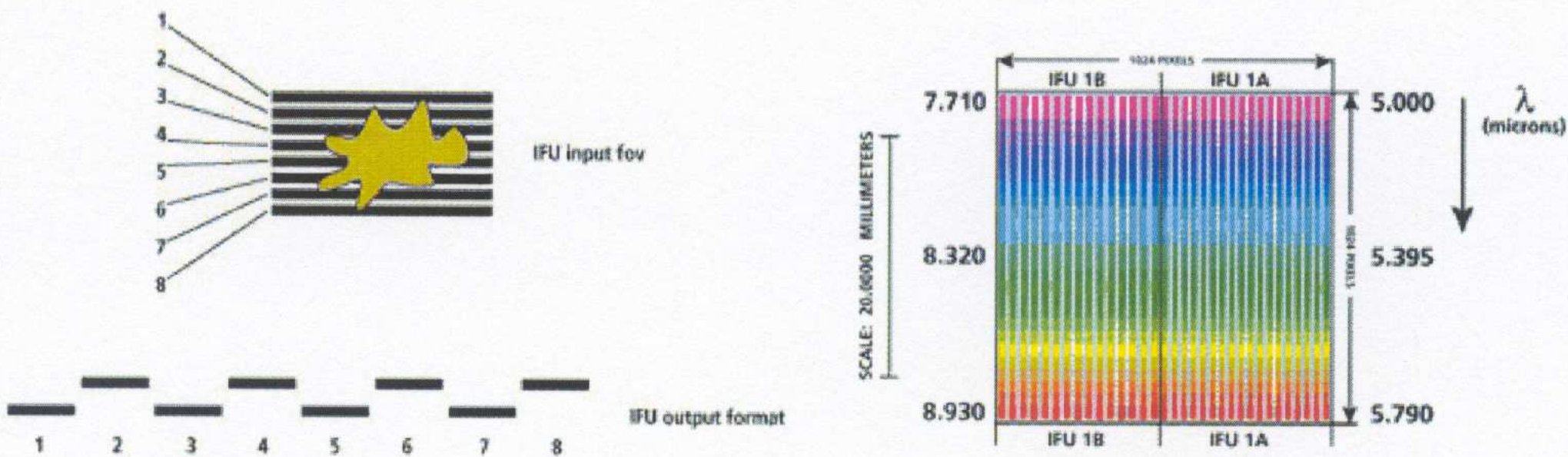


Figure 50. Schematic illustration of the MIRI IFU image slicer format (left) and dispersed spectra on detector (right)

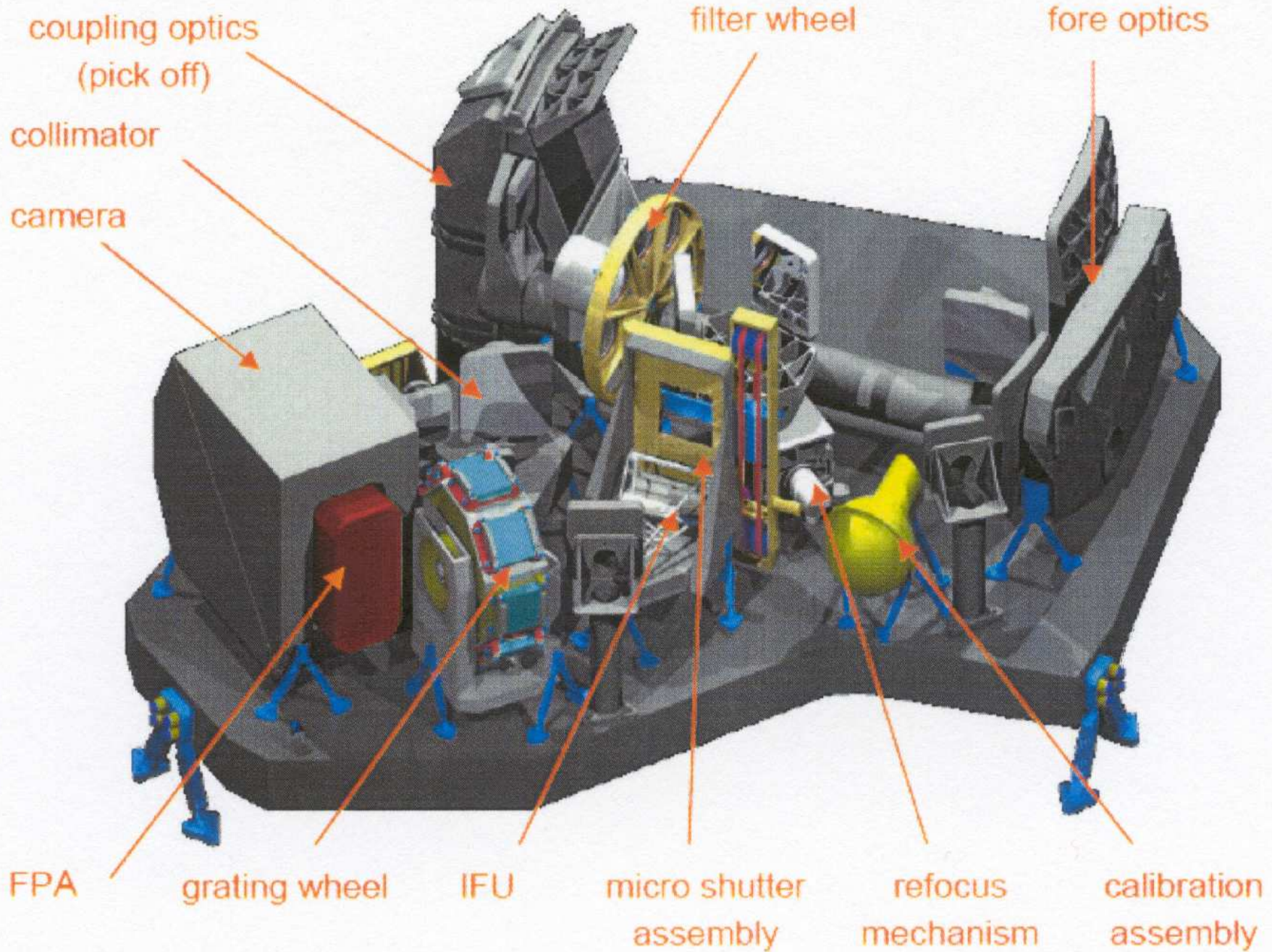


Figure 45. The NIRSpec instrument.

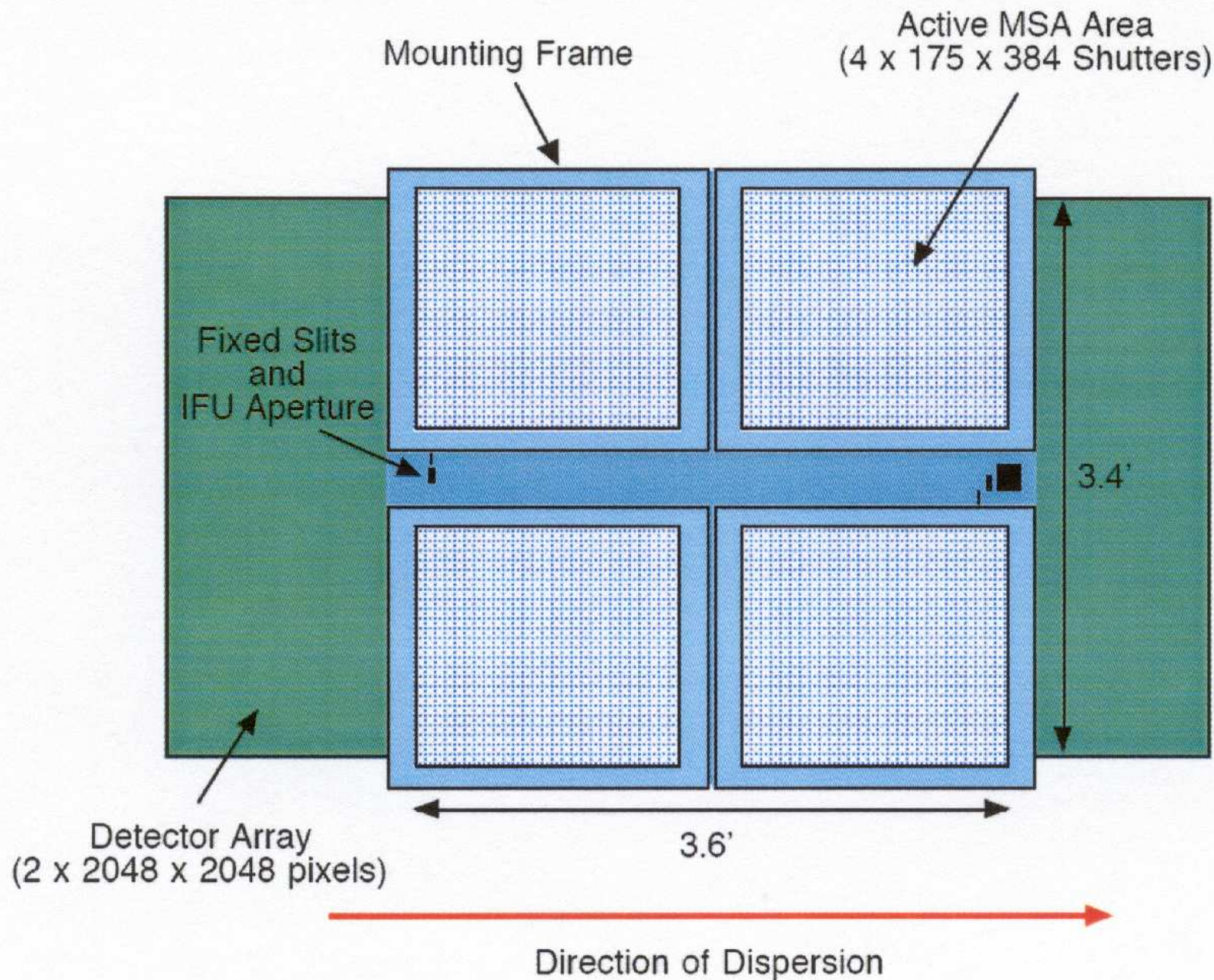


Figure 46. Schematic layout of the NIRSpec slit mask overlaid the detector array projected to the same angular scale.

Table 11. Science Instrument Characteristics

| Instrument | Wavelength (μm) | Optical Elements | FPA | Plate Scale (milliarcsec/ pixel) | Field of View |
|---------------------------------------|---------------------------------|---------------------------------------------------------------------------------------------------------------------------------------------------------|-------------------------------------|----------------------------------------|---------------------------------------------|
| NIRCam (Short Wavelength) | 0.6 - 2.3 | fixed filters (R~4, R~10, R~100), coronagraphic spots | Two 2×2 mosaics of 2048×2048 arrays | 32 | 2.2×4.4 arcmin |
| NIRCam (Long Wavelength) ¹ | 2.4 - 5.0 | fixed filters (R~4, R~10, R~100), coronagraphic spots | Two 2048×2048 arrays | 65 | 2.2×4.4 arcmin |
| NIRSpec (prism, R=100) | 0.6 - 5.0 | Transmissive slit mask: four 384×175 micro-shutter array, 250 (spectral) by 500 (spatial) milliarcsec; fixed slits 200 or 300 mas wide by 4 arcsec long | Two 2048×2048 arrays | 100 | 3.4×3.1 arcmin |
| NIRSpec (grating, R=1000) | 1.0-5.0 | | | | |
| NIRSpec (IFU, R=3000) | 1.0-5.0 | Integral field unit | 1024×1024 | 110 | 3.0×3.0 arcmin |
| MIRI (imaging) | 5 - 27 | Broad-band filters, coronagraphic spots & phase masks | | | |
| MIRI (prism spectroscopy) | 5 - 10 | R ~ 100 | Two 1024×1024 arrays | 200 to 470 | 1.4×1.9 arcmin (26×26 arcsec coronographic) |
| MIRI (spectroscopy) | 5 - 27 | Integral field spectrograph (R~3000) in 4 bands | | | |
| TFI (Short-wavelength) | 1.2 - 2.4 | Order-blocking filters+etalon (R~100) | 2048×2048 | 68 | 2.3×2.3 arcmin |
| TFI (Long-wavelength) ² | 2.5 - 4.8 | Order-blocking filters+etalon (R~100) | 2048×2048 | 68 | 2.3×2.3 arcmin |

NOTE: ¹Use of a dichroic renders the NIRCam long-wavelength field of view co-spatial with the short wavelength channel, and the two channels acquire data simultaneously.

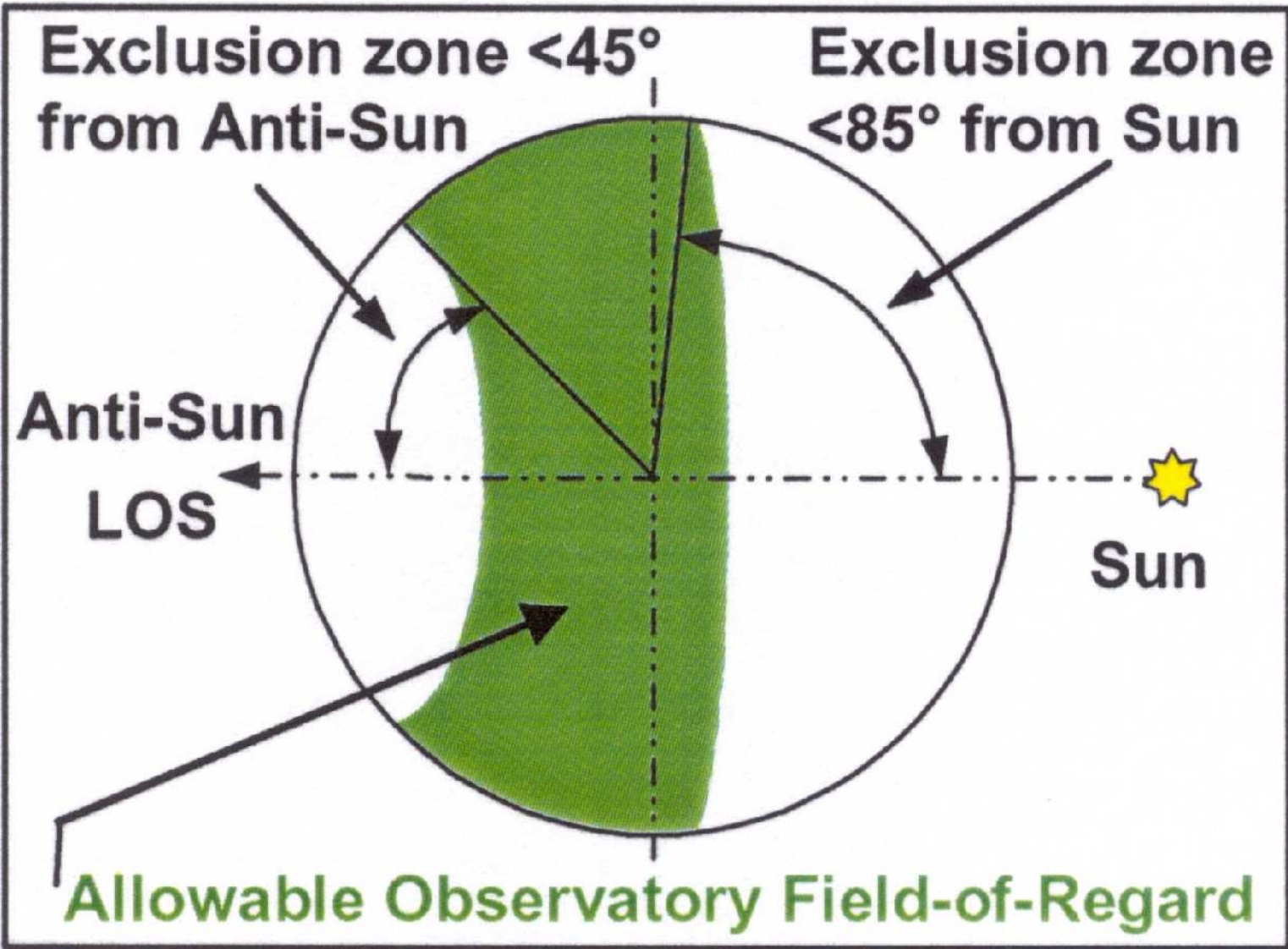


Figure 30. Observatory field of regard (FOR).

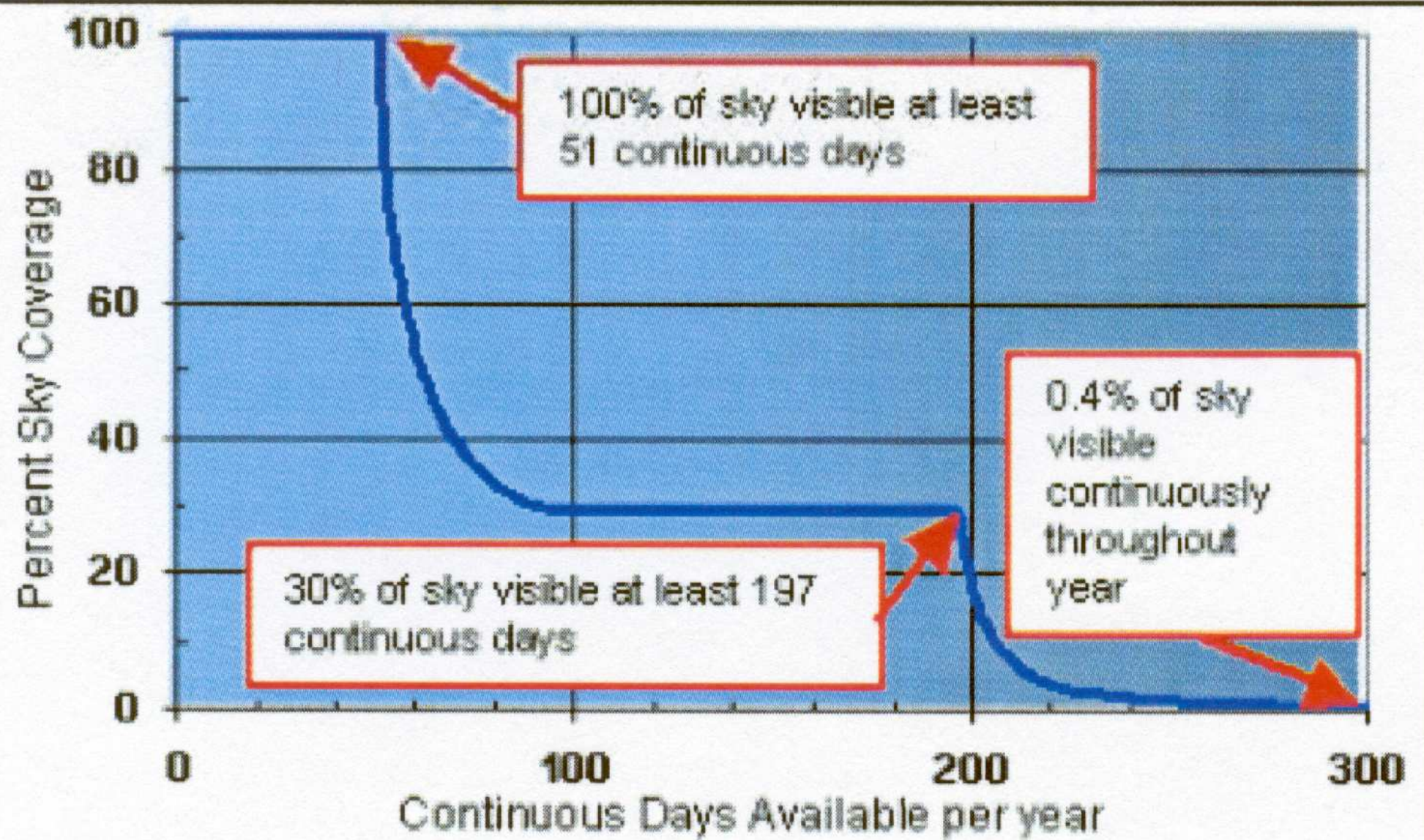
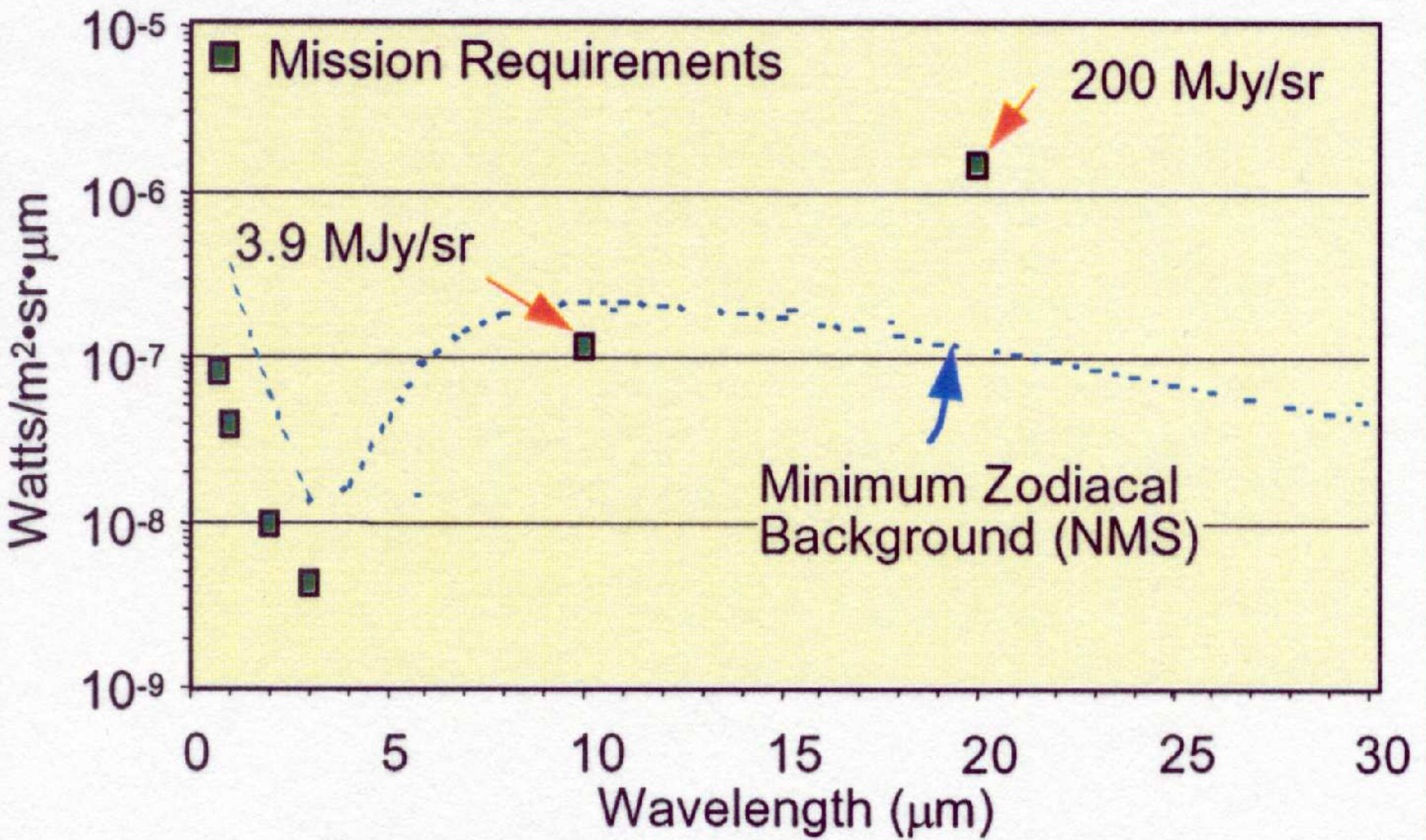


Figure 29. Sky coverage and continuous visibility.



| | |
|---------------------------------------------|--------------------------------------------------------------------------------------------------------------------------------------------------------------------------------------------------------|
| Telescope FOV | ~ 166 square arcminutes FOV. ISIM instruments share FOV with common aperture |
| Orbit | Lissajous orbit about L2 |
| Celestial Sphere Coverage | <p>100% annually</p> <p>39.7% at any given time</p> <p>100% of sphere has at least 51 contiguous days visibility</p> <p>30% for > 197 days</p> <p>Continuous within 5 degrees of ecliptic poles</p> |
| Overall Observing Efficiency | Observatory ~ 80.7% |
| Mission Life | <p>5-year minimum lifetime</p> <p>11 years for fuel</p> <p>Commissioning in less than 6 months</p> |
| Schedule | August 2011 launch |

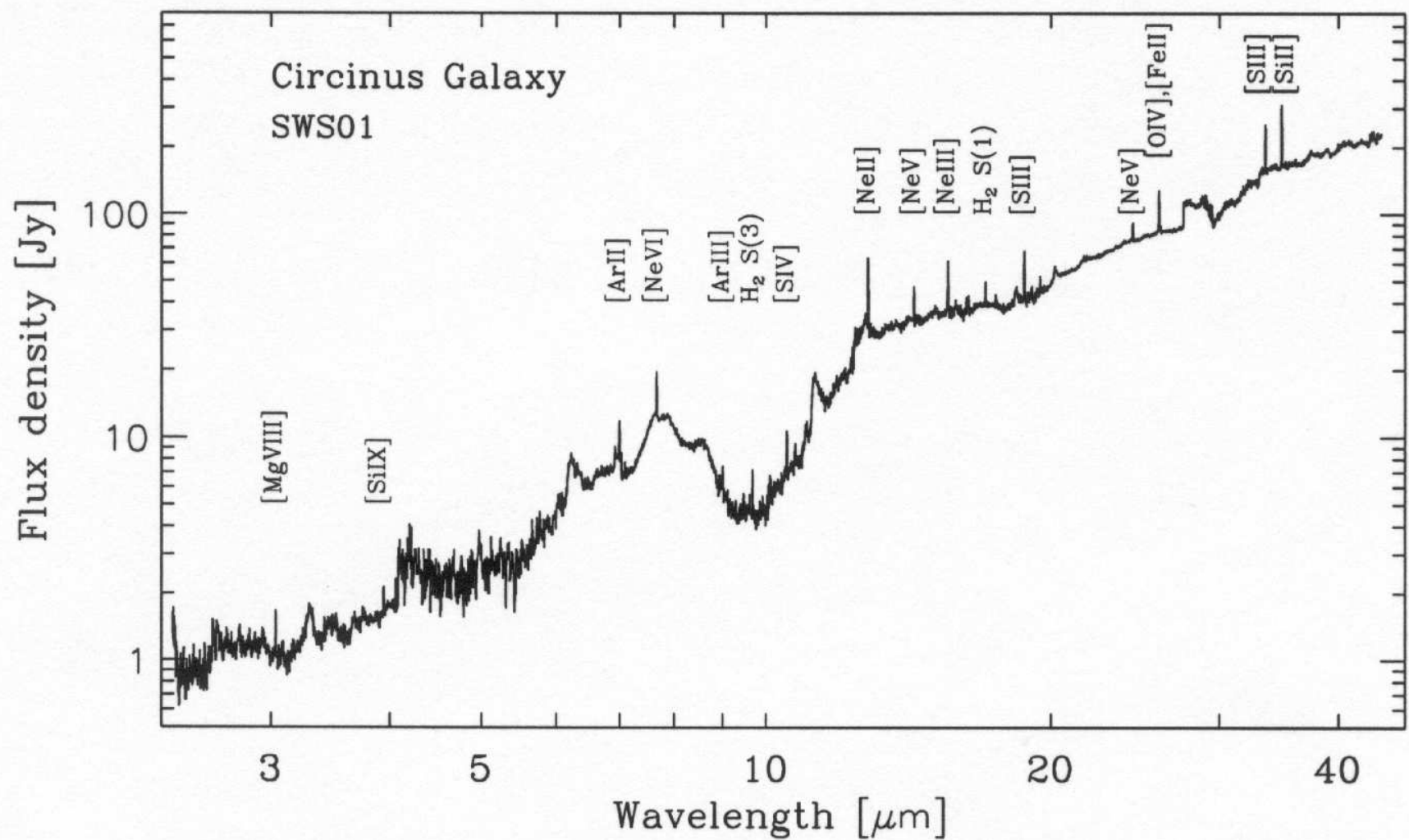


Figure 9. ISO Circinus Spectrum. Mid-infrared spectrum of the Circinus galaxy taken with ISO shows an abundance of emission lines useful for diagnosing the energy sources which power ULIRGs (From Moorwood et al. 1996).

Table 6. Required Sensitivity Values

| Wave-length (μm) | Instrument / Mode | Sensitivity | Equivalents |
|----------------------------------|---------------------|----------------------------------------------------------------------------------------------------|----------------------------------------------------------|
| 1.1 | NIRCam | $1.21 \times 10^{-34} \text{ Wm}^{-2}\text{Hz}^{-1}$ SN=10 in 10,000 s or less and R=4 bandwidth | 12.1 nJy, AB=28.7 |
| 2 | NIRCam | $1.04 \times 10^{-34} \text{ Wm}^{-2}\text{Hz}^{-1}$ SN=10 in 10,000 s or less and R=4 bandwidth | 10.4 nJy, AB=28.9 |
| 3.5 | TFI | $3.68 \times 10^{-33} \text{ Wm}^{-2}\text{Hz}^{-1}$ SN=10 in 10,000 s or less and R=100 bandwidth | 368 nJy, AB=25.0 |
| 3.0 | NIRSpec/ Low Res | $1.2 \times 10^{-33} \text{ Wm}^{-2}\text{Hz}^{-1}$ SN=10 in 10,000 s or less and R=100 bandwidth | 120 nJy, AB=26.2 |
| 2.0 | NIRspec/ Med Res | $5.2 \times 10^{-22} \text{ Wm}^{-2}$ SN=10 in 100,000 s or less and R=1000 bandwidth | $5.2 \times 10^{-19} \text{ erg s}^{-1} \text{ cm}^{-2}$ |
| 10 | MIRI/ Broad-Band | $7.0 \times 10^{-33} \text{ Wm}^{-2}\text{Hz}^{-1}$ SN=10 in 10,000 s or less and R=5 bandwidth | 700 nJy, AB=24.3 |
| 21 | MIRI/ Broad-Band | $7.3 \times 10^{-32} \text{ Wm}^{-2}\text{Hz}^{-1}$ SN=10 in 10,000 s or less and R=4.2 bandwidth | 7.3 μJy , AB=21.7 |
| 9.2 | MIRI/ Spect. | $1.0 \times 10^{-20} \text{ Wm}^{-2}$ SN=10 in 10,000 s or less and R=2400 bandwidth | $1.0 \times 10^{-17} \text{ erg s}^{-1} \text{ cm}^{-2}$ |
| 22.5 | MIRI/ Spect. | $5.6 \times 10^{-20} \text{ Wm}^{-2}$ SN=10 in 10,000 s or less and R=1200 bandwidth | $5.6 \times 10^{-17} \text{ erg s}^{-1} \text{ cm}^{-2}$ |

Note: "Sensitivity" is defined to be the brightness of a point source detected with the signal-to-noise ratio and integration time specified. Targets at the North Ecliptic Pole are assumed.

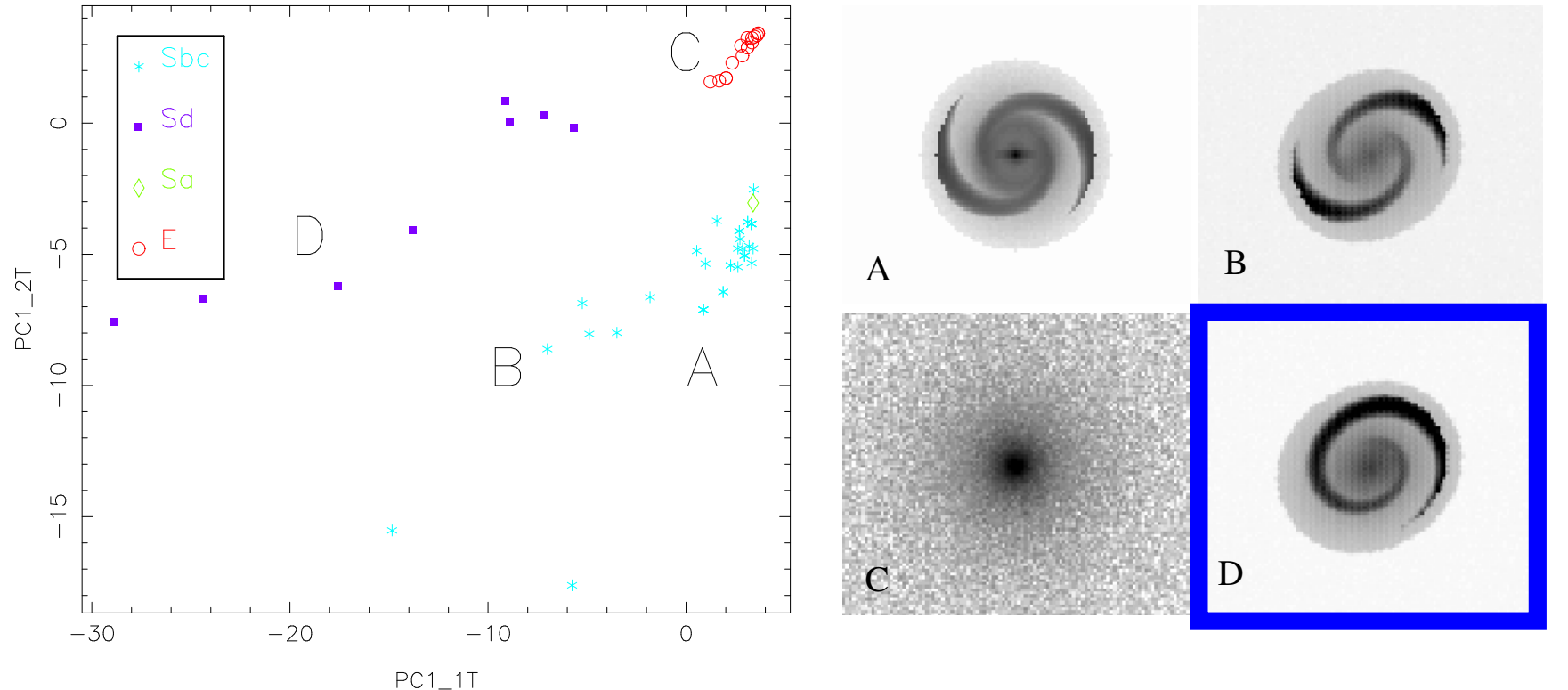
Table 1. JWST Measurements for the End of the Dark Ages Theme

| Observation | Primary Instrument | Magnitude or flux | Target Density |
|--------------------------------------|--------------------|----------------------------------------------------------------------|------------------------|
| Ultra-deep survey, SNe | NIRCam | AB = 31 mag | 1 arcmin ⁻² |
| In-depth study | NIRSpec | AB = 28 mag, R~100 | 1 arcmin ⁻² |
| | MIRI | AB = 28 mag | 1 arcmin ⁻² |
| Ly α forest diagnostics | NIRSpec | 2×10^{-19} erg cm ⁻² s ⁻¹ , R~1000 | Individual |
| Transition in Ly α properties | TFI | 2×10^{-19} erg cm ⁻² s ⁻¹ , R~1000 | 1 arcmin ⁻² |
| Transition in Ly α /Balmer | NIRSpec | 2×10^{-19} erg cm ⁻² s ⁻¹ , R~1000 | 1 arcmin ⁻² |
| Measure ionizing continuum | NIRSpec | 2×10^{-19} erg cm ⁻² s ⁻¹ , R~1000 | 1 arcmin ⁻² |
| Ionization source nature | NIRSpec | | |
| | MIRI | | |
| LF of dwarf galaxies | NIRCam | AB = 31 mag | |

Table 2. JWST Measurements for the Assembly of Galaxies Theme

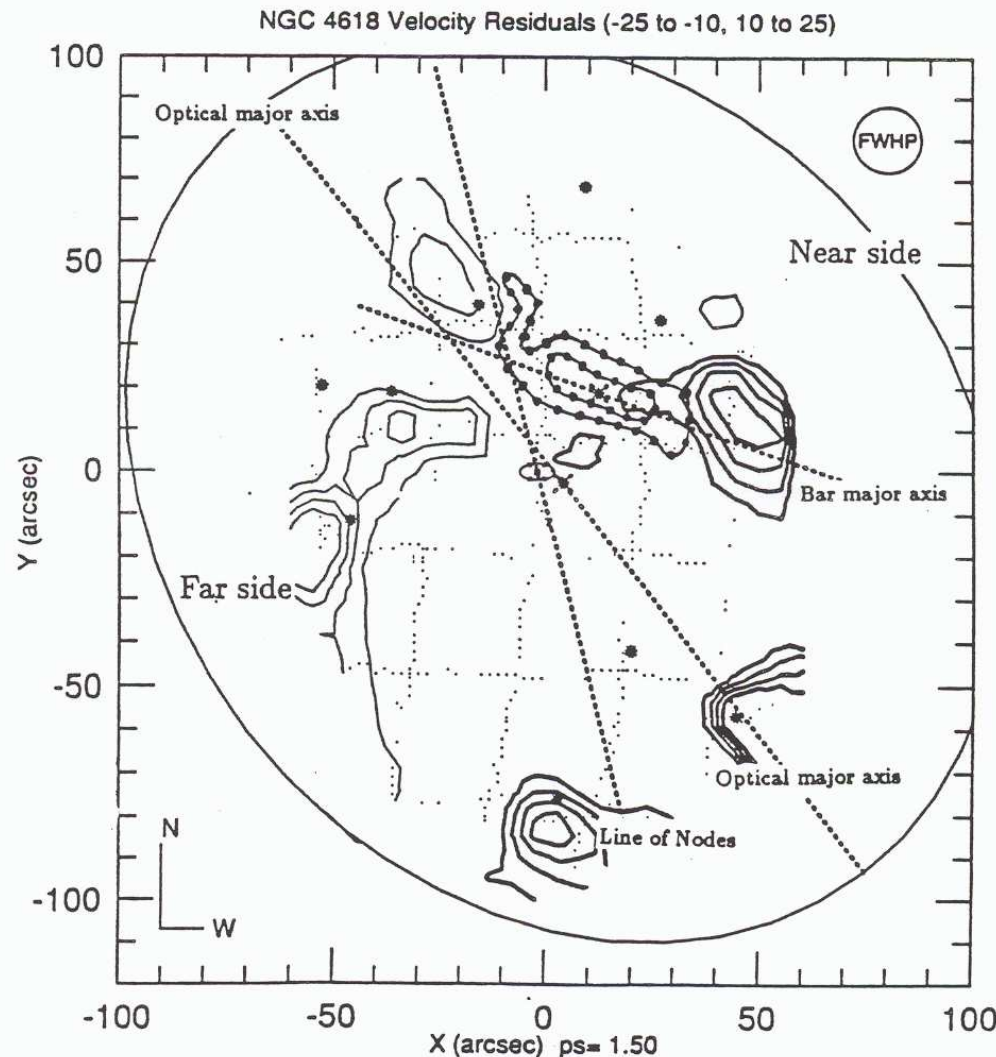
| Topic | Primary Instrument | Key Observation | Magnitude or Flux | Target Density |
|--------------------------------------------|--------------------------------------|--------------------------------------------------------------------------------------------------------------|--------------------------------------------------------|---------------------------|
| Faint galaxy identification and morphology | NIRCam | Detect the SMC at $z = 5$ in rest-frame V | $L_{AB} = 30.3$ mag | 100 arcmin^{-2} |
| Metallicity determination | NIRSpec | Determine R_{23} from emission line ratios for galaxy with $\text{SFR} = 3 M_{\odot}/\text{yr}$ at $z = 5$ | $5 \times 10^{-19} \text{ erg s}^{-1} \text{ cm}^{-2}$ | 100 arcmin^{-2} |
| Scaling relations | MIRI spectroscopy (short wavelength) | Measure stellar velocity dispersion for $R_{AB}=24.5$ Lyman Break galaxy at $z = 3$ | $AB(9\mu\text{m}) = 21.3$ mag | 1 arcmin^{-2} |
| Obscured galaxies | MIRI spectroscopy (long wavelength) | Measure [NeVI] in ULIRG with Arp220 L_{bol} assuming Circinus spectrum | $1.4 \times 10^{-19} \text{ W m}^{-2}$ | Individual |

Quantitative Morphology – We can numerically describe and identify $m=1$ galaxies!



Odewahn et.al. 2002 ApJ, 568, 539

Fourier Decomposition is remarkably good in distinguishing and quantifying bars and (1-armed, 2-armed) spiral structure. JWST will be able to do this out to $z=5$ at least, hence enabling to quantitatively trace galaxy assembly.



H α Kinematics in NGC 4618 (Odewahn 1990)

Substantial departures
from circular motion
in $m=1$ arms, OFTEN
accompanied by large
OB associations (SSC?)

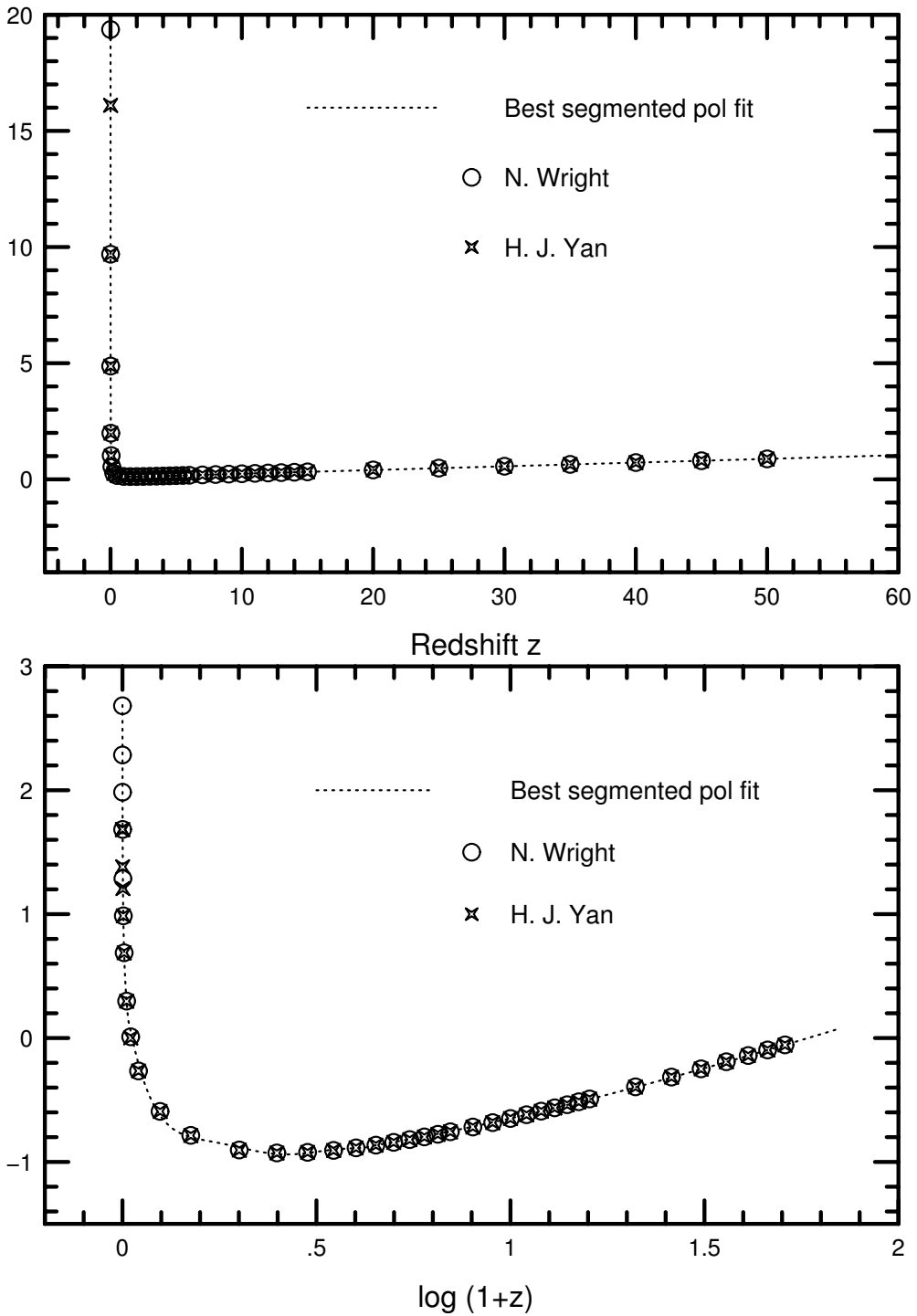
Spatially resolved NIRSpec and MIRI integral-field spectra of distant galaxies when compared to the quantitative structure from NIRCam Fourier Decompositions, will directly trace the physical causes of locally enhanced star-formation: infall, bulk velocities in excess of regular rotation, etc.

(5) Details on JWST image simulations:

- All based on HST/WFPC2 F300W images from the HST mid-UV survey of nearby galaxies (Windhorst et al. 2002,ApJ Suppl. 143, 113).
- WMAP COSMOLOGY: $H_0=71 \text{ km/s/Mpc}$, $\Omega_m=0.27$, $\Omega_\Lambda=0.73$.
- INSTRUMENT: 6.0 m effective aperture, diffraction limited at $\lambda \gtrsim 2.0 \mu\text{m}$, JWST/NIRCam, $0''.034/\text{pix}$, read-noise=5.0 e⁻, dark-current=0.02 e⁻/s, NEP-Sky(1.6 μm)=21.7 mag/($''^2$) in L2, Zodi spectrum, $t_{exp}=4 \times 900\text{s}$.

| Row | Telesc. | Redshift | $\lambda (\mu\text{m})$ | FWHM ($''$) |
|-----|---------|------------|-------------------------|---------------|
| 1 | HST | $z \sim 0$ | $0.293 \mu\text{m}$ | $0''.04$ |
| | JWST | $z=1.0$ | $0.586 \mu\text{m}$ | $0''.084$ |
| | JWST | $z=2.0$ | $0.879 \mu\text{m}$ | $0''.084$ |
| 2 | JWST | $z=3.0$ | $1.17 \mu\text{m}$ | $0''.084$ |
| | JWST | $z=5.0$ | $1.76 \mu\text{m}$ | $0''.084$ |
| | JWST | $z=7.0$ | $2.34 \mu\text{m}$ | $0''.098$ |
| 3 | JWST | $z=09.0$ | $2.93 \mu\text{m}$ | $0''.122$ |
| | JWST | $z=12.0$ | $3.81 \mu\text{m}$ | $0''.160$ |
| | JWST | $z=15.0$ | $4.69 \mu\text{m}$ | $0''.197$ |

Theta-z relation for $H_0=71$, $\Omega_m=0.27$, $\Omega_\Lambda=0.73$



Angular size vs. redshift relation in a Lambda dominated cosmology of $H_0 = 71 \text{ km s}^{-1} \text{ Mpc}^{-1}$, $\Omega_m=0.27$, $\Omega_\Lambda=0.73$.

In the top panel the relation is nearly linear in $1/z$ for $z \lesssim 0.05$ (the small angle approximation) and linear in z for $z \gtrsim 3$ (the Lambda dominated universe).

All curvature occurs in the range $0.05 \lesssim z \lesssim 3$, which is coded up in the IRAF script that does the JWST simulations.

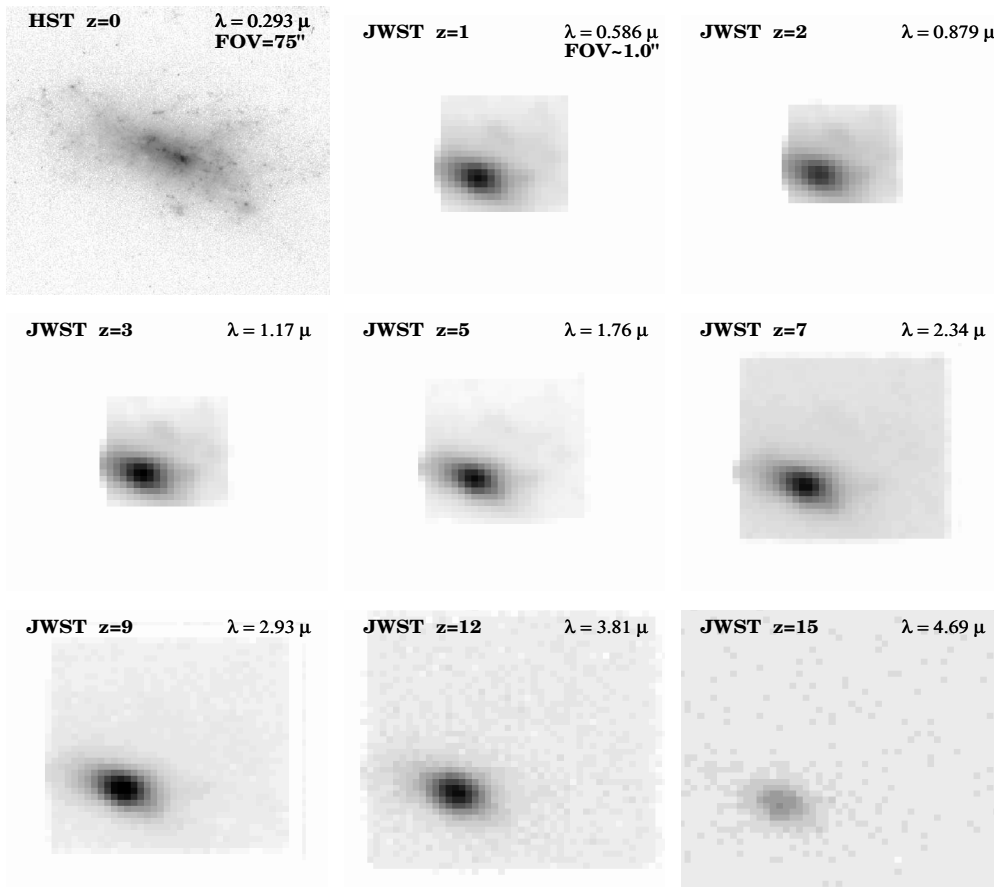


Fig. 4.01. JWST simulations based on HST/WFPC2 F300W images of the dwarf irregular NGC1140 ($z=0.0050$). This compact high SB object would be visible to $z\simeq15$, but hard to classify at all $z\geq1$.

ASSUMPTIONS: COSMOLOGY: $H_0=71$ km/s/Mpc, $\Omega_m=0.27$, and $\Omega_\Lambda=0.73$.

INSTRUMENT: 6.0 m effective aperture, JWST/NIRCam, $0.034''/\text{pix}$, $RN=5.0 \text{ e}^-$, $\text{Dark}=0.020 \text{ e}^-/\text{sec}$, NEP $H\text{-band Sky}=21.7 \text{ mag/arcsec}^2$ in L2, Zodiacal spectrum, $t_{exp}=1.0 \text{ hrs}$, read-out every 900 sec.

Row 1: $z=0.0$ (HST $\lambda=0.293\mu\text{m}$, FWHM= $0.04''$), $z=1.0$ (JWST $\lambda=0.586\mu\text{m}$, FWHM= $0.084''$), and $z=2.0$ (JWST $\lambda=0.879\mu\text{m}$, FWHM= $0.084''$).

Row 2: $z=3.0$ (JWST $\lambda=1.17\mu\text{m}$, FWHM= $0.084''$), $z=5.0$ (JWST $\lambda=1.76\mu\text{m}$, FWHM= $0.084''$), and $z=7.0$ (JWST $\lambda=2.34\mu\text{m}$, FWHM= $0.098''$).

Row 3: $z=9.0$ (JWST $\lambda=2.93\mu\text{m}$, FWHM= $0.122''$), $z=12.0$ (JWST $\lambda=3.81\mu\text{m}$, FWHM= $0.160''$), and $z=15.0$ (JWST $\lambda=4.69\mu\text{m}$, FWHM= $0.197''$)

The compact high-SB dwarf irregular galaxy NGC1140 ($z=0.0050$).

With JWST, this object would be visible to $z\simeq15$, but it will be hard to classify at all redshifts $z\geq1$.

Note that the object indeed reaches a minimum angular size at $z\simeq1.7$.

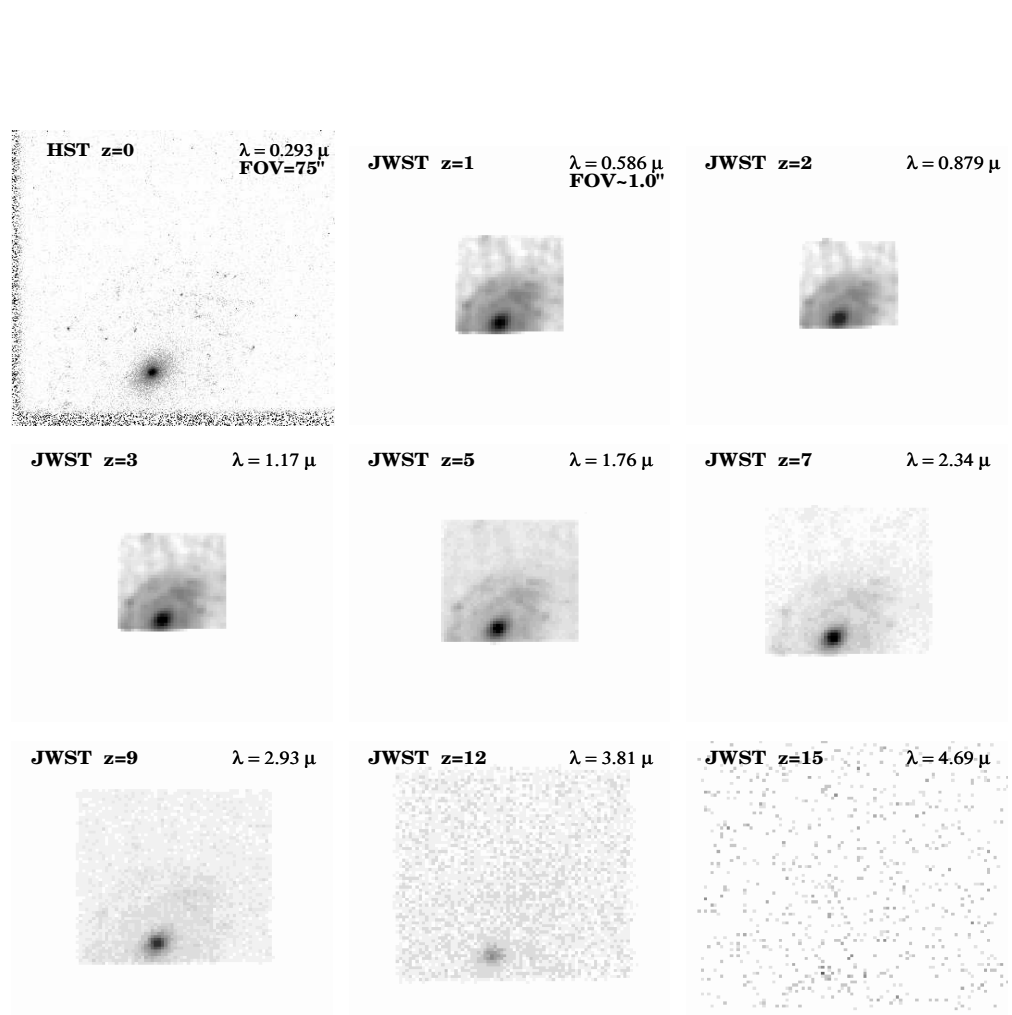


Fig. 4.02. JWST simulations based on HST/WFPC2 F300W images of the mid-type spiral NGC2551 (0.0078). Such an object would be visible to $z \approx 10$, but only recognizable to $z \approx 7$.

ASSUMPTIONS: COSMOLOGY: $H_0 = 71$ km/s/Mpc, $\Omega_m = 0.27$, and $\Omega_\Lambda = 0.73$.

INSTRUMENT: 6.0 m effective aperture, JWST/NIRCam, $0.034''/\text{pix}$, $RN = 5.0 \text{ e}^-$, $\text{Dark} = 0.020 \text{ e}^-/\text{sec}$, NEP H-band Sky = 21.7 mag/arcsec² in L2, Zodiacal spectrum, $t_{\text{exp}} = 1.0$ hrs, read-out every 900 sec.

Row 1: $z=0$ (HST $\lambda=0.293\mu\text{m}$, FWHM = $0.04''$), $z=1.0$ (JWST $\lambda=0.586\mu\text{m}$, FWHM = $0.084''$), and $z=2.0$ (JWST $\lambda=0.879\mu\text{m}$, FWHM = $0.084''$).

Row 2: $z=3.0$ (JWST $\lambda=1.17\mu\text{m}$, FWHM = $0.084''$), $z=5.0$ (JWST $\lambda=1.76\mu\text{m}$, FWHM = $0.084''$), and $z=7.0$ (JWST $\lambda=2.34\mu\text{m}$, FWHM = $0.098''$).

Row 3: $z=9.0$ (JWST $\lambda=2.93\mu\text{m}$, FWHM = $0.122''$), $z=12.0$ (JWST $\lambda=3.81\mu\text{m}$, FWHM = $0.160''$), and $z=15.0$ (JWST $\lambda=4.69\mu\text{m}$, FWHM = $0.197''$)

The mid-type spiral NGC2551 ($z=0.0078$) would be visible out to $z \approx 10$, but only recognizable out to $z \approx 7$.

Its disk is in principle visible to $z \gtrsim 5-7$. Hence, if such objects are not seen by JWST at $z \lesssim 3$, then disks likely form at $z \lesssim 3$.

With HST we have seen glimpses of this, but with JWST these will become robust conclusions.

ST z=0

$\lambda = 0.293 \mu$
FOV=75"

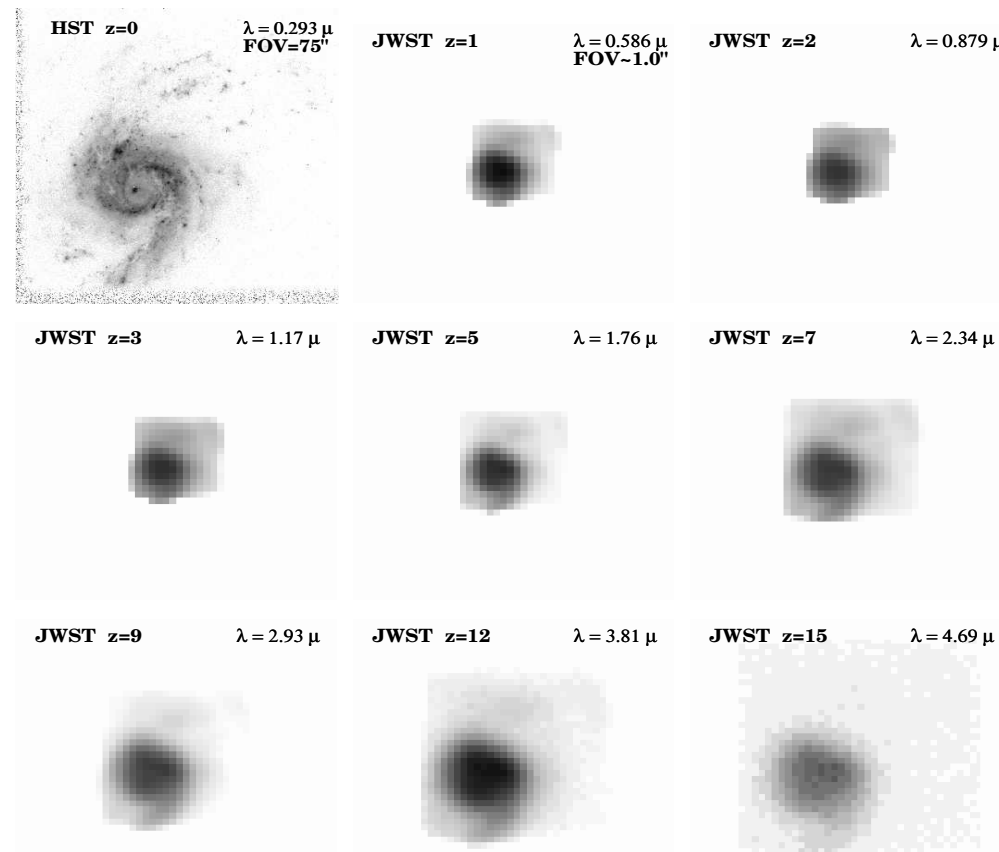


Fig. 4.03. JWST simulations based on HST/WFPC2 F300W images of the high-SB starbursting dwarf spiral galaxy NGC3310 (0.0033). The minimum in the Θ -z relation at $z \simeq 1.7$ and the JWST diffraction limit at $\lambda \geq 2.2 \mu\text{m}$ — combined with the object's very high rest-frame UV SB — conspire to improve the effective JWST resolution on the mid-UV morphology of this object from $z \simeq 2$ to $z \simeq 7$.

ASSUMPTIONS: COSMOLOGY: $H_0=71 \text{ km/s/Mpc}$, $\Omega_m=0.27$, and $\Omega_\Lambda=0.73$. INSTRUMENT: 6.0 m effective aperture, JWST/NIRCam, $0.034''/\text{pix}$, $RN=5.0 \text{ e}^-$, Dark= $0.020 \text{ e}^-/\text{sec}$, NEP H-band Sky= $21.7 \text{ mag/arcsec}^2$ in L2, Zodiocal spectrum, $t_{exp}=1.0 \text{ hrs}$, read-out every 900 sec.

Row 1: $z=0.0$ (HST $\lambda=0.293 \mu\text{m}$, FWHM= $0.04''$), $z=1.0$ (JWST $\lambda=0.586 \mu\text{m}$, FWHM= $0.084''$), and $z=2.0$ (JWST $\lambda=0.879 \mu\text{m}$, FWHM= $0.084''$). **Row 2:** $z=3.0$ (JWST $\lambda=1.17 \mu\text{m}$, FWHM= $0.084''$), $z=5.0$ (JWST $\lambda=1.76 \mu\text{m}$, FWHM= $0.084''$), and $z=7.0$ (JWST $\lambda=2.34 \mu\text{m}$, FWHM= $0.098''$). **Row 3:** $z=9.0$ (JWST $\lambda=2.93 \mu\text{m}$, FWHM= $0.122''$), $z=12.0$ (JWST $\lambda=3.81 \mu\text{m}$, FWHM= $0.160''$), and $z=15.0$ (JWST $\lambda=4.69 \mu\text{m}$, FWHM= $0.197''$)

The very high-SB, compact starbursting dwarf spiral galaxy NGC3310 ($z=0.0033$).

The minimum in the Θ -z relation at $z \simeq 1.7$ and the JWST diffraction limit at $\lambda \geq 2.2 \mu\text{m}$ — combined with the object's very high rest-frame UV-SB — conspire to improve the effective JWST resolution on the mid-UV morphology of this object from $z \simeq 2$ to $z \simeq 7$.

A rather exceptional case of where nasty cosmology doesn't appear to cost you prohibitive sensitivity, but gains you resolution!

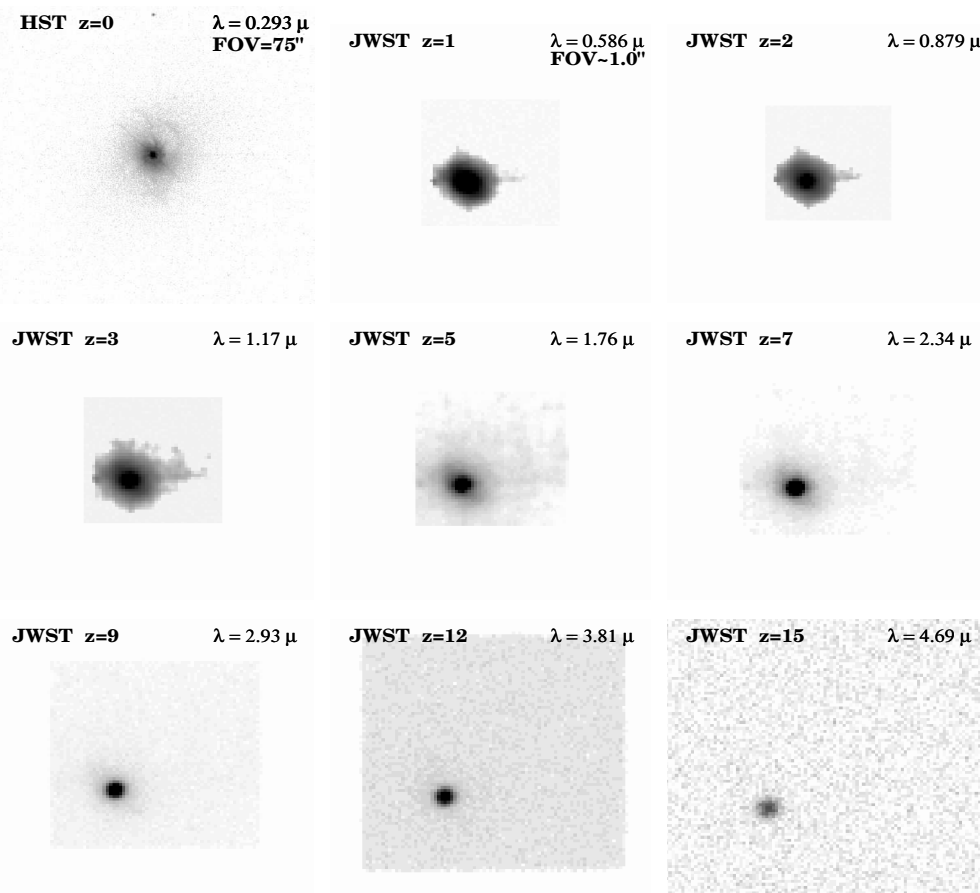


Fig. 4.04. JWST simulations based on HST/WFPC2 F300W images of the Seyfert galaxy NGC3516 (0.0088). Note that the faint nebulosity surrounding the AGN in the mid-UV at $z=0$ essentially disappears at $z \geq 7$, so that at high redshifts such objects would look like a pure AGN.

ASSUMPTIONS: COSMOLOGY: $H_0=71$ km/s/Mpc, $\Omega_m=0.27$, and $\Omega_\Lambda=0.73$.

INSTRUMENT: 6.0 m effective aperture, JWST/NIRCam, $0.034''/\text{pix}$, $RN=5.0\text{ e}^-$, $\text{Dark}=0.020\text{ e}^-\text{/sec}$, NEP H-band Sky=21.7 mag/arcsec² in L2, Zodiacal spectrum, $t_{exp}=1.0$ hrs, read-out every 900 sec.

Row 1: $z=0.0$ (HST $\lambda=0.293\mu\text{m}$, FWHM= $0.04''$), $z=1.0$ (JWST $\lambda=0.586\mu\text{m}$, FWHM= $0.084''$), and $z=2.0$ (JWST $\lambda=0.879\mu\text{m}$, FWHM= $0.084''$). **Row 2:** $z=3.0$ (JWST $\lambda=1.17\mu\text{m}$, FWHM= $0.084''$), $z=5.0$ (JWST $\lambda=1.76\mu\text{m}$, FWHM= $0.084''$), and $z=7.0$ (JWST $\lambda=2.34\mu\text{m}$, FWHM= $0.098''$). **Row 3:** $z=9.0$ (JWST $\lambda=2.93\mu\text{m}$, FWHM= $0.122''$), $z=12.0$ (JWST $\lambda=3.81\mu\text{m}$, FWHM= $0.160''$), and $z=15.0$ (JWST $\lambda=4.69\mu\text{m}$, FWHM= $0.197''$)

The Seyfert galaxy NGC3516 ($z=0.0088$) has a faint nebulosity surrounding its AGN in the mid-UV, while at longer wavelengths the surrounding elliptical galaxy is present (not shown here).

The nebulosity surrounding the AGN is essentially SB-dimmed away at $z \geq 7$, so that at high redshifts these objects would look like purely stellar objects (“quasars”).

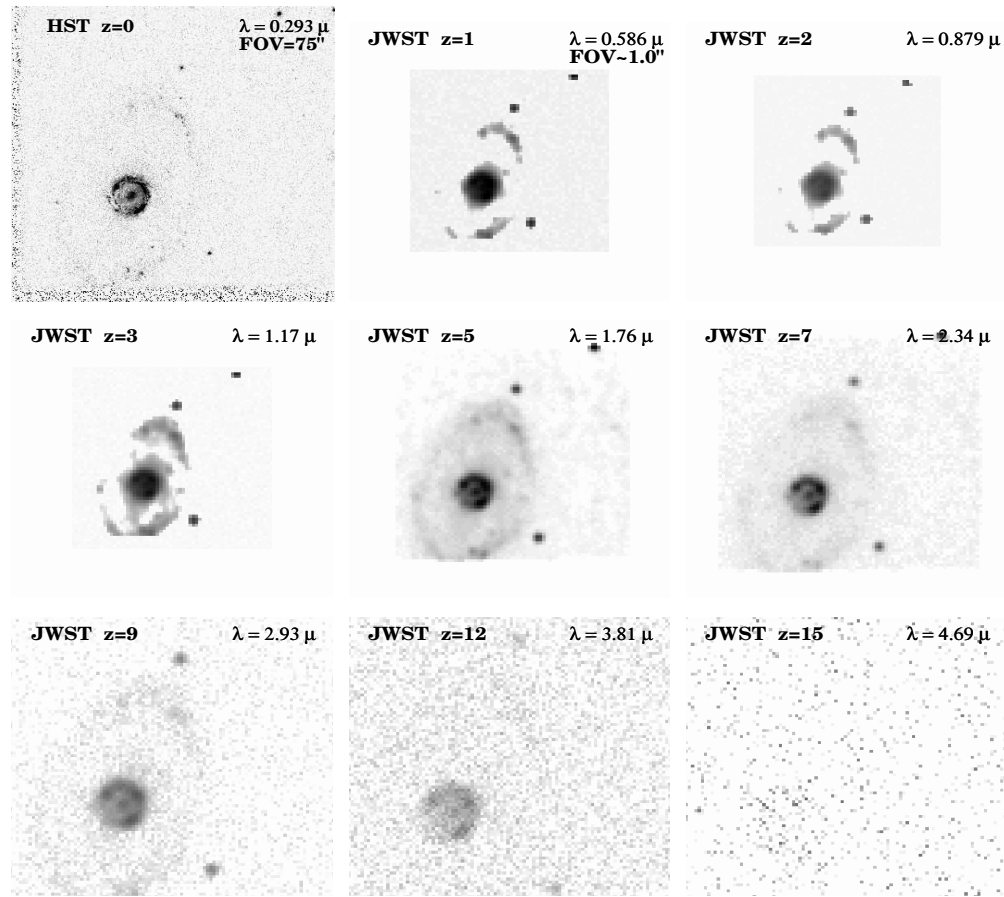


Fig. 4.05. JWST simulations based on HST/WFPC2 F300W images of the barred ring galaxy NGC6782 (0.0125). Note again that for $z \simeq 2$ –7, the effective resolution on the bright star-forming ring improves with increasing redshift, until the $(1+z)^4$ -dimming completely kills it for $z \gtrsim 10$.

ASSUMPTIONS: COSMOLOGY: $H_0=71 \text{ km/s/Mpc}$, $\Omega_m=0.27$, and $\Omega_\Lambda=0.73$.

INSTRUMENT: 6.0 m effective aperture, JWST/NIRCam, $0.034''/\text{pix}$, $RN=5.0 \text{ e}^-$, $\text{Dark}=0.020 \text{ e}^-/\text{sec}$, NEP H-band Sky=21.7 mag/arcsec² in L2, Zodiacal spectrum, $t_{exp}=1.0 \text{ hrs}$, read-out every 900 sec.

Row 1: $z=0.0$ (HST $\lambda=0.293\mu\text{m}$, FWHM= $0.04''$), $z=1.0$ (JWST $\lambda=0.586\mu\text{m}$, FWHM= $0.084''$), and $z=2.0$ (JWST $\lambda=0.879\mu\text{m}$, FWHM= $0.084''$). **Row 2:** $z=3.0$ (JWST $\lambda=1.17\mu\text{m}$, FWHM= $0.084''$), $z=5.0$ (JWST $\lambda=1.76\mu\text{m}$, FWHM= $0.084''$), and $z=7.0$ (JWST $\lambda=2.34\mu\text{m}$, FWHM= $0.098''$). **Row 3:** $z=9.0$ (JWST $\lambda=2.93\mu\text{m}$, FWHM= $0.122''$), $z=12.0$ (JWST $\lambda=3.81\mu\text{m}$, FWHM= $0.160''$), and $z=15.0$ (JWST $\lambda=4.69\mu\text{m}$, FWHM= $0.197''$)

The barred ring galaxy NGC6782 (0.0125) shows that at $z \simeq 2$ to $z \simeq 7$, the effective resolution on its high-SB bright star-forming ring improves with increasing redshift, until the $(1+z)^4$ -dimming completely kills it for $z \gtrsim 10$ –12.

Another good case showing why cosmology is not “WYSIWYG”.